

1 Grapevine pruning time affects natural wound colonization by wood- 2 invading fungi

3
4 **María del Pilar Martínez-Diz^{1,2}, Ales Eichmeier³, Milan Spetik³, Rebeca Bujanda⁴, Ángela
5 Díaz-Fernández¹, Emilia Díaz-Losada¹, David Gramaje^{4,*}**

6
7 ¹Estación de Viticultura e Enoloxía de Galicia (AGACAL-EVEGA), Ponte San Clodio s/n
8 32428-Leiro-Ourense, Spain.

9 ²Universidade da Coruña, Facultade de Ciencias, Zapateira, 15071 A Coruña, Spain.

10 ³Mendel University in Brno, Faculty of Horticulture, Mendeleum - Institute of Genetics,
11 Valticka 334, 69144, Lednice, Czech Republic.

12 ⁴Instituto de Ciencias de la Vid y del Vino (ICVV), Consejo Superior de Investigaciones
13 Científicas - Universidad de la Rioja - Gobierno de La Rioja, Ctra. LO-20 Salida 13, Finca La
14 Grajera, 26071 Logroño, Spain.

15
16 * Corresponding author. Instituto de Ciencias de la Vid y del Vino (ICVV), Consejo Superior
17 de Investigaciones Científicas, Universidad de la Rioja, Gobierno de La Rioja, Ctra. LO-20
18 Salida 13, 26007 Logroño, Spain.

19 E-mail address: david.gramaje@icvv.es (D. Gramaje)

20 21 22 **ABSTRACT**

23 Grapevine pruning wounds made during the dormant season are a port of entry of wood-
24 invading fungi. Timing of pruning may affect the wound susceptibility to these fungi, such as
25 those associated with grapevine trunk diseases (GTDs). This study aimed to determine the effect
26 of pruning time on natural fungal infection in six vineyards in Galicia, Spain, belonging to three
27 Denominations of Origin (D.O) over two growing seasons. Pruning wounds were left
28 unprotected physically and chemically during two periods of three months each, from
29 November to February and from February to May. The diversity and composition of the fungal
30 microbiome that colonized the pruning wounds was identified by ITS2 high-throughput
31 amplicon sequencing (HTAS). A broad range of fungi was able to colonize grapevine pruning
32 wounds at both infection periods. Fungal microbiome composition did not shift as year of
33 sampling. Fungal communities were affected in their diversity and composition by the D.O.,
34 whereas the spatial variation (i.e. vineyard within each region) was low. Pruned canes
35 harboured a core community of fungal species, which appeared to be independent of the
36 infection period. Accumulated rainfall over 8 and 11 weeks after pruning positively correlated
37 with the total fungal microbiome and in particular with the GTD fungal genus *Diaporthe*
38 abundances. A strong seasonal effect on GTD fungal infection was detected for most genera,
39 with higher percentages of abundance detected after pruning in February (winter) as compared
40 with that of pruning in November (mid-autumn). In light of the GTD colonization results and
41 given the environmental conditions and the geographical location of this study, early pruning
42 is recommended to reduce the infections caused by GTD fungi during the pruning season in
43 Galicia.

44
45 **Keywords:** Culture-independent analysis, fungal microbiome, grapevine trunk diseases, High-
46 throughput amplicon sequencing, *Vitis vinifera*

51 1. Introduction

52
53 The most important operation during the dormant season in vineyards is pruning. Pruning
54 of grapevines is recommended any time after leaf fall, which may occur late fall or throughout
55 the winter. The purpose of pruning is to obtain maximum yields of high-quality grapes and to
56 allow adequate vegetative growth for the following season (Jackson, 2004). Timing of pruning
57 within the dormant season may affect the grapevine phenology, and thus yield and fruit quality
58 (Zheng et al., 2017). Early or late pruning can also affect the susceptibility of the plant to abiotic
59 disorders, such as spring frost (Jackson, 2004), or the pruning wound susceptibility to infections
60 caused by wood-invading fungi, such as those associated with grapevine trunk diseases (GTDs)
61 (Luque et al., 2014).

62 Grapevine trunk diseases are caused by a broad range of taxonomically unrelated fungal
63 pathogens that infect woody tissues. They reduce longevity and productivity of grapevines and
64 thereby cause substantial economic losses to industry (Gramaje et al., 2018). To date, up to 135
65 fungal species belonging to 35 genera have been associated with GTDs worldwide (Gramaje et
66 al., 2018; Aigon-Mouhous et al., 2019; Lawrence et al., 2019; Berlanas et al., 2020), thus
67 accounting for the largest group of fungi known to infect grapevines (Gramaje et al., 2018).
68 GTDs are mainly caused by fungal ascomycetes but some basidiomycetous fungi are also
69 thought to play a relevant role in this pathosystem (Fischer, 2002; Cloete et al., 2015; Brown et
70 al., 2020). GTD fungal spores can infect grapevines through any open wound, including those
71 caused by de-suckering, trimming and re-training (Makatini et al., 2014). Nonetheless, annual
72 pruning wounds are the primary point of infection providing many entry sites each growing
73 season throughout the life of a vineyard (Gramaje et al., 2018).

74 The main GTDs in mature vines are *Eutypa dieback*, *Botryosphaeria dieback*, *Phomopsis*
75 *dieback* and *esca* disease (Gramaje et al., 2018). In North America, several *Cytospora* spp. have
76 also been recently reported causing dieback and wood cankers in grapevine (Lawrence et al.,
77 2017). Grapevine pathogens responsible for these diseases are mainly spread through the
78 dispersion of airborne spores. Previous studies showed that spore release and thus, high risk
79 periods of infection vary during the growing season depending on the geographical location
80 and fungal pathogen but mainly overlay with dormant pruning seasons in both the Southern and
81 Northern Hemispheres (Pearson, 1980; Petzoldt et al., 1983; Eskalen and Gubler, 2001;
82 Amposah et al., 2009; Trouillas, 2009; Úrbez-Torres et al., 2010; van Niekerk et al., 2010;
83 Valencia et al., 2015). Pruning wounds susceptibility to GTD pathogens primarily depends on
84 the pruning time and the period elapsed between pruning and possible infection cases. Studies
85 using artificial spore inoculations indicate that susceptibility of grapevine pruning wound
86 significantly decreases as the length of time between pruning and inoculation increases, with
87 seasonal variation noted between regions, due mainly to climatic differences (Moller and
88 Kasimatis, 1980; Munkvold and Marois, 1995; Eskalen et al., 2007; Serra et al., 2008; Úrbez-
89 Torres and Gubler, 2011; van Niekerk et al., 2011; Ayres et al., 2016).

90 The rate of natural fungal microbiome infections in pruned canes has been poorly studied
91 so far, and data available is only referred in the context of GTD pathogens infections in France
92 (Lecomte and Bailey, 2011) and northeast Spain (Luque et al., 2014). These studies employed
93 standard culture-dependent microbial techniques; however, these approaches tend to
94 underestimate species richness and misrepresent fungal activity, because fungi may be highly
95 selective, hidden and slow growing. Molecular-based methods have progressively replaced
96 morphological techniques to characterize the microbiome in nature. These methods allow the
97 detection and identification of a greater number of microorganisms, including species that are
98 unable to be isolated in culture (Amann et al., 1995). The novel advances in high-throughput
99 sequencing (HTS) technology have increased both the resolution and scope of fungal

100 community analyses and have revealed a highly diverse and complex fungal microbiome of
101 plant vascular systems (Studholme et al., 2011).

102 In recent years, grapevine has become a plant model system for microbiome research. HTS
103 tools have been actively used to map the microbiome on grapevine organ epiphytes (i.e., root,
104 leaf and berry) because of its importance with grape production and specially with regards to
105 foliar and fruit diseases control along with the biological implication of indigenous
106 microorganisms with the local signature of a wine (Bokulich et al., 2014; Perazzolli et al., 2014;
107 Zarronaindia et al., 2015). Identification of the microbial communities inhabiting the
108 grapevine endosphere has been achieved using standard culture-dependent microbial
109 techniques (West et al., 2010; Compant et al., 2011; Baldan et al., 2014; Kraus et al., 2019).
110 Culture-independent high-throughput amplicon sequencing (HTAS) approaches have recently
111 been used to improve the microbiome profiling of grapevine woody organs such as cane and
112 trunk (Faist et al., 2016; Deyett et al., 2017; Dissanayake et al., 2018; Eichmeier et al., 2018).

113 In this study, we tested the following hypotheses: (1) the diversity and composition of fungal
114 microbiome that colonizes grapevine pruning wounds changes according to the pruning time
115 and this shift is related to environmental conditions; (2) the susceptibility of pruning wounds to
116 fungal infection and the ability of GTD pathogens to colonize them depend on the pruning time,
117 therefore this would allow us to make pruning recommendations to growers in the short term
118 in order to avoid high pathogen infection periods. The objective was therefore to identify the
119 diversity and composition of the fungal microbiome, in particular GTD fungi, infecting pruning
120 wounds in six mature vineyards at two pruning times over two years by HTAS: (i) after an early
121 pruning in autumn; and (ii) after a late pruning in winter. In addition, we investigated the
122 relationship between the main weather data recorded during the experimental period and the
123 rate of fungal colonization.

124

125 **2. Materials and methods**

126

127 *2.1. Location and characteristics of the experimental vineyards*

128

129 Experiments were conducted at six experimental plots located in three Denominations of
130 Origin (D.O. Valdeorras, D.O. Ribeiro and D.O. Rías Baixas; two experimental plots per D.O.)
131 in Galicia region, Spain (Table S1), from November 2017 to May 2019. Plots within each D.O.
132 were <10 km apart and had very similar climates. Standard cultural practices were employed in
133 all sites during the grapevine growing season, and the management of powdery and downy
134 mildews was performed using only wettable sulphur and copper compounds and applied at label
135 dosages and following IPM guidelines, respectively, if required. Plots of 1,500 vines in these
136 vineyards have been monitored biannually for the evolution of GTD symptoms since 2014 to
137 the present. At the time this study was started (2017), about 12% of vines had shown symptoms
138 of trunk diseases in previous monitoring dates. The main symptoms of GTDs observed during
139 monitoring included chlorotic leaves, stunted shoots, and short internodes (*Eutypa dieback*),
140 the arm and cordon death (*Botryosphaeria*, *Eutypa* and *Phomopsis diebacks*) and tiger-pattern
141 foliar necrosis (*esca*). All vineyards were trained as bilateral cordons with spur pruning (Royat).
142 Grapevine cultivars differed among D.O. (Table S1), so data from each D.O. was analysed
143 independently due to the previously reported variable degree of susceptibility of each grapevine
144 cultivar to fungal trunk pathogen infections (Martínez-Diz et al., 2019a). The experimental plots
145 were located <6km to automatic weather stations owned by MeteoGalicia (Weather Service of
146 Galician Regional Government, Xunta de Galicia). Data obtained from the weather station in
147 each D.O. were considered to be representative of the two experimental plots.

148

149 *2.2 Pruning and sampling*

150 A total of 200 vines were pruned in each experimental plot in mid-autumn (between 13 and
151 14 November for both years and experimental plots) leaving six buds. Then, 25 pruned canes
152 in each vineyard were chosen at random and labelled for subsequent samplings. Wood of these
153 25 canes were taken to the laboratory for DNA extraction. Three months later in winter
154 (between 21 and 22 February for both years and experimental plots), a 15-cm section was cut
155 from the labelled 25 pruned canes and removed from their upper end and taken to the laboratory
156 for DNA extraction. On the same day of this sampling, all the vines were pruned to four buds.
157 A longer than usual wood section (5–7 cm) was left above the top bud. Three months later in
158 spring (between 22 and 23 May for both years and experimental plots), sampling for DNA
159 extraction from approximately a 15-cm wood section was repeated following the same
160 procedure earlier, and the labelled canes were definitely pruned to two buds. All canes were
161 therefore exposed to natural infections for three months after pruning (infection period 1:
162 November-February; infection period 2: February-May). Pruning scissors were disinfested with
163 70% ethanol every pruning cut. Pruning wounds were not protected physically nor chemically
164 during the experiment.

165

166 *2.3. DNA extraction and sequencing*

167

168 Before DNA extraction, pruned canes were sequentially washed in 70% ethanol and sterile
169 distilled water. Upon this treatment, bark was carefully peeled out from the upper ends of canes
170 with a flame-sterilised scalpel to expose the inner tissues starting from the pruning wound. The
171 3-mm end was cut and discarded to avoid bias by the colonization of saprophytic fungal species.
172 DNA was extracted from 0.5 g of xylem tissue collected between 3- to 8-mm from the pruning
173 wound using the i-genomic Plant DNA Extraction Mini Kit (Intron Biotechnology, South
174 Korea). DNA yields from each sample were quantified using the Invitrogen Qubit 4
175 Fluorometer with Qubit dsDNA HS Assay (Thermo Fisher Scientific, Waltham, USA), and the
176 extracts were adjusted to 10-15 ng/ μ L. After DNA quantification, samples of each pruning time
177 and vineyard were pooled in groups of five, resulting in a total of five replicates for every batch
178 of 25 canes. A total of 180 DNA samples was analysed. Complete fungal ITS2 region (around
179 300 bp) was amplified using the primers ITS86F (5' GTGAAT CATCGAATCTTTGAA 3')
180 (Turenne et al., 1999) and ITS4 (5' TCCTCCGCTTATTGATATGC 3') (White et al., 1990), to
181 which the Illumina sequencing primer sequences were attached to their 5' ends. PCRs were
182 carried out in a final volume of 25 μ L, containing 2.5 μ L of template DNA, 0.5 μ M of the
183 primers, 12.5 μ L of Supreme NZYtaq 2x Green Master Mix (NZYTech, Lisboa, Portugal),
184 and ultrapure water up to 25 μ L. The reaction mixture was incubated as follows: initial
185 denaturation at 95 °C for 5 min, followed by 35 cycles of 95 °C for 30 s, 49 °C for 30 s, 72 °C
186 for 30 s, and a final extension step at 72 °C for 10 minutes. The oligonucleotide indices which
187 are required for multiplexing different libraries in the same sequencing pool were attached in a
188 second PCR round with identical conditions but only five cycles and 60 °C as the annealing
189 temperature for a schematic overview of the library preparation process. A negative control that
190 contained no DNA was included in every PCR round to check for contamination during library
191 preparation (BPCR). The libraries were run on 2 % agarose gels stained with GreenSafe
192 (NZYTech, Lisboa, Portugal) and imaged under UV light to verify the library size. Libraries
193 were purified using the Mag-Bind RXNPure Plus magnetic beads (Omega Biotek, Norcross,
194 GA, USA), following the instructions provided by the manufacturer. Then, they were pooled in
195 equimolar amounts according to the quantification data provided by the Qubit dsDNA HS
196 Assay (Thermo Fisher Scientific, Waltham, USA). The pool was sequenced in a MiSeq PE300
197 run (Illumina, San Diego, USA). An additional negative control was included during the
198 extraction step. A positive control containing DNA of a grapevine endorhizosphere sample
199 previously evaluated by ITS HTAS was also included (Martínez-Diz et al., 2019b). All control

200 samples were prepared for sequencing to evaluate potential contaminations of the entire
201 process.

202

203 *2.4. Data analysis of the high-throughput amplification assay*

204

205 Sequence quality was visualized using FastQC-0.10.1 (Andrews, 2010), and the CLC Genomics
206 Workbench 6.5.1 (CLC Bio, Aarhus, Denmark) was used to trim and merge the paired end
207 reads. The parameter Q30 was applied and only reads longer than 100 nts with average read
208 quality > 30 were considered for further analysis. Q30 represents the quality score of a base,
209 also known as a Phred or Q score. It is an integer value representing the estimated probability
210 of an error. Q30 number means base call accuracy 99.9%. The distance of evaluated reads in
211 the trimming and merging step was set from 200 to 400 nts. Primer and Illumina adapter
212 sequences were also trimmed out. The reads were exported to fasta format by CLC Genomics
213 Workbench 6.5.1 (CLC Bio, Aarhus, Denmark).

214 Exported fasta files were used for clustering in SCATA (<https://scata.mykopat.slu.se/>).
215 Parameters for clustering were: Clustering distance 0.015; Minimum alignment to consider
216 clustering 0.95; Mismatch penalty 0.1; Gap open penalty 0; Gap extension penalty 1; End gap
217 weight 0; Collapse homopolymers 3; Downsample sample size 0; Remove low frequency
218 genotypes 0; Tag-by-Cluster Max 10000000; Blast E-value cutoff 1e-60; Cluster engine
219 USERACH; Number of repseqs to report 50. The CBS isolates were used as a reference
220 sequences. Singleton operational taxonomic units (OTUs) were discarded. The sequences of
221 non-singleton OTUs were used as the representative sequence and were identified using the
222 blastn algorithm using the GenBank/NCBI reference database (version 2.2.30+). OTUs with no
223 kingdom-level classification or matching chloroplast, mitochondrial or Viridiplantae sequences
224 were excluded from the dataset. In order to optimize the dataset, each sample was rarefied to
225 the same sequence number per sample, that is, 21,287 fungal sequences. OTUs represented
226 globally by less than five reads were discarded (Glynnou et al., 2018). The resulting quality
227 dataset was used for the estimation of richness and diversity. The metadata, OTUs table and
228 associated taxonomic classifications deployed in this study have been deposited in figshare (ID:
229 79113). HTAS data were deposited in GenBank/NCBI under BioProject Acc. No.
230 PRJNA625395.

231

232 *2.5. Fungal diversity, taxonomy distribution and statistical analysis*

233

234 Within sample type, alpha-diversity estimates were calculated by analyzing the Shannon
235 diversity and Chao1 richness in Phyloseq package, as realized in the tool MicrobiomeAnalyst
236 (Dhariwal et al., 2017). Multiple mean comparisons using Tukey's test were performed to
237 determine how fungal alpha-diversity differed among year, D.O., vineyard within each D.O.,
238 and pruning time. *P* values were corrected for multiple comparisons using the sequential
239 Bonferroni correction. Relationship in OTUs composition among samples were investigated by
240 calculating Bray Curtis metrics, and visualized by means of PCoA plots (Vázquez-Baeza et al.,
241 2013) using MicrobiomeAnalyst. PERMANOVA was performed to investigate which OTUs
242 significantly differed in abundance among experimental factors. Rarefaction curves and Good's
243 coverage values were calculated using MicrobiomeAnalyst.

244 The Linear Discriminant Analysis Effect Size (LEfSe) algorithm was used to identify taxa
245 (genus level or higher) that differed in relative abundance between pruning times (Segata et al.,
246 2011). The online MicrobiomeAnalyst interface was used, the threshold for the logarithmic
247 Linear Discriminant Analysis (LDA) score was set at 1.0 and the Wilcoxon *p*-value at 0.05.
248 The results are displayed in a bar graph. The fungal OTUs shared among compartments were

249 obtained by a Venn-diagram analysis using the software retrieved from
250 <http://bioinformatics.psb.ugent.be>.

251 In order to compare the percentage of abundance of each fungal genus associated with
252 GTDs between both infection periods, an analysis of variance with log transforms was used.
253 Normality of residuals was checked by Shapiro-Wilk's test, and homogeneity of variances
254 by Levene's test. Means were compared with Tukey's Honestly Significant Difference range
255 test ($P \leq 0.05$) using Statistix 10 software (Analytical Software).

256

257 2.6. Correlation with weather variables

258

259 The number of OTUs corresponding to the total fungal microbiome, and the fungal genera
260 associated with GTDs was correlated with the main weather data (daily mean relative
261 humidity, daily mean temperature and accumulated rainfall). Values from the number of
262 OTUs were transformed by $\log(n/N * 1000 + 1)$. Where n was the number of OTUs detected
263 on each sample and N was the total number of OTUs detected. Temperature and humidity
264 records were averaged over 1, 2, 4, 8, and 11 weeks post-pruning periods. Rainfall records
265 were accumulated and log-transformed to make data conform to normality over the same
266 periods. Spearman's correlation coefficients were calculated using the function *cor* of the
267 'stats' package of R v. 3.6.0 (R Core Team, 2019).

268

269 3. Results

270

271 3.1. High-throughput amplicon sequencing

272

273 After paired-end alignments, quality filtering and deletion of chimeras, singletons, a total of
274 10,740,761 fungal internal transcribed spacer (ITS2) sequences were generated from 180
275 samples, excluding controls, and assigned to 259 fungal OTUs.

276 OTUs generated from the negative control used in the amplification step belonged to 30
277 genera. The number of sequences of each OTU present in the negative control was subtracted
278 from the sequence abundance of that OTU in the experimental samples according to Nguyen et
279 al. (2015). No contamination was detected in the negative control used in the DNA extraction
280 step. Good's coverage values in all samples ranged from 99.25 to 100%, capturing nearly all
281 the diversity with an adequate sequencing depth (Figure S1). Chao1 diversity estimator ranged
282 from 5 to 26, while Shannon diversity estimator ranged from 0.31 to 2.27 (Table S2).

283

284 3.2. Fungal communities differed among Denominations of Origin

285

286 The alpha-diversity of fungal communities differed among D.O. (Chao1: $P = 0.0047$,
287 Shannon: $P < 0.001$; Fig 1), and principal coordinates analysis (PCoA) of Bray Curtis data
288 demonstrated that D.O. was the primary source of beta-diversity ($R^2 = 0.48$, $P < 0.001$) (Fig.
289 2). Therefore, data of each D.O. was analysed independently.

290 The relative abundance of fungal phyla, order and family detected across all D.O. is shown
291 in Fig. S2. Considering the three D.O., the most abundant phyla were Ascomycota, followed
292 by Basidiomycota (Fig. S2a). The most abundant orders were Dothideales, followed by
293 Capnodiales and Pleosporales (Fig. S2b). The most abundant families were Dothioraceae,
294 followed by Cladosporiaceae and Dermateaceae (Fig. S2c). Comparing the fungal microbiota
295 of the three D.O., 56.8% of fungal OTUs were shared among them (Fig. 3). Specific OTUs
296 associated with each vineyard ranged from 12.1 to 18.4% of their fungal communities (Fig. 3).

297 In D.O. Rías Baixas, the most abundant families were Dothioraceae (62.9%), followed by
298 Cladosporiaceae (10.2%) and Pleosporaceae (9.9%) (Fig. S2c). The most abundant families in
299 D.O. Ribeiro were Cladosporiaceae (26.5%), followed by Dothioraceae (21.6%) and
300 Dermateaceae (12.1%). In D.O. Valdeorras, the most abundant families were Dothioraceae
301 (51.8%), followed by Cladosporiaceae (19.9%) and Tremellaceae (4.5%).

302

303 *3.3. Fungal diversity exhibits a temporal variation over the infection periods*

304

305 Alpha-diversity of fungal communities in grapevine wood samples did not differ
306 significantly between experimental plots (Fig. S3) and year (Fig. S4) within each D.O. (Table
307 1), thus the data of both years and experimental plots were combined for analyses. Comparing
308 the microbiome in the grapevine inner tissue at the three sampling times (1: November, 2:
309 February and 3: May), higher fungal diversity was mostly observed towards the sampling time
310 3 ($P < 0.05$) (Fig. S5). Excluding the initial fungal microbiome estimated in November, and
311 considering the two infection periods, fungal community diversity was significantly different
312 between both periods in D.O. Rías Baixas (Table 1; Fig. 4b). A PCoA further demonstrated that
313 variation in the D.O. Rías Baixas dataset could be attributed to infection periods ($R^2 = 0.60$;
314 Fig. S6b). In D.O. Ribeiro, the infection periods did not predict Shannon diversity (Table 1;
315 Fig. 4a), and any summary metrics of alpha-diversities in D.O. Valdeorras (Table 1; Fig. 4c).
316 Infection periods did not affect the Bray Curtis metric of beta-diversity in D.O. Ribeiro and
317 D.O. Valdeorras ($R^2 < 0.40$; Fig. S6b and S6c).

318 The relative abundance of fungal families detected across sampling times is shown in Fig.
319 5. In D.O. Ribeiro, the most abundant families were Cladosporiaceae (34.2%), Dothioraceae
320 (33.1%) and Sporidiobolaceae (6.3%) (initial microbiome); Cladosporiaceae (22.9%),
321 Dothioraceae (18.4%) and Dermateaceae (14.6%) (infection period 1); and Cladosporiaceae
322 (22.2%), Dothioraceae (15.1%) and Dermateaceae (14.9%) (infection period 2). In D.O. Rías
323 Baixas, the most abundant families were Dothioraceae (81.3%), Cladosporiaceae (9.9%) and
324 Pleosporaceae (4.4%) (initial microbiome); Dothioraceae (66.5%), Cladosporiaceae (9.4%) and
325 Pleosporaceae (7.1%) (infection period 1); and Dothioraceae (26.9%), Pleosporaceae (20.4%)
326 and Dermateaceae (8.3%) (infection period 2). In D.O. Valdeorras, the most abundant families
327 were Dothioraceae (70.9%), Cladosporiaceae (23.1%) and Filobasidiaceae (1.2%) (initial
328 microbiome); Dothioraceae (45.2%), Cladosporiaceae (17.8%) and Tremellaceae (8.5%)
329 (infection period 1); and Dothioraceae (40.2%), Cladosporiaceae (20.9%) and Dermateaceae
330 (12.8%) (infection period 2).

331

332 *3.4. Infection periods specific and shared fungal assemblages*

333

334 The percentage of shared fungal OTUs among the three sampling times were similar in all
335 D.O.: 31.5% (D.O. Ribeiro), 31.4% (D.O. Rías Baixas), and 28.7% (D.O. Valdeorras) (Fig. 6).
336 Specific OTUs associated with each sampling time ranged from 15.8 to 21.4% (D.O. Ribeiro),
337 from 6.9 to 23.8% (D.O. Rías Baixas), and from 9.7 to 17.2% (D.O. Valdeorras). Excluding the
338 initial fungal microbiome and comparing the two infection periods, shared fungal OTUs among
339 infection periods were also similar: 54.1% (D.O. Ribeiro), 56.3% (D.O. Rías Baixas), and
340 56.0% (D.O. Valdeorras). The OTUs that were unique in both infection periods for each D.O.
341 are shown in Table S3. Genera *Eucasphaeria* and *Penicillium* were unique to the infection
342 period November-February, while *Cryptodiaporthe* genus was unique to the infection period
343 February-May in the three D.O.

344 The linear discriminant analysis effect size (LEfSe) detected 3, 9 and 4 fungal clades in the
345 grapevine inner tissues, which discriminated the fungal communities between infection periods
346 in D.O. Ribeiro, D.O. Rías Baixas and D.O. Valdeorras, respectively (Fig. 7). The infection

347 period 2 showed higher number of differentially abundant fungal clades (2, 8, and 3 in D.O.
348 Ribeiro, D.O. Rías Baixas and D.O. Valdeorras, respectively). In the infection period 1, the
349 dominant fungal genus in all D.O. was *Aureobasidium*. In the infection period 2, the dominant
350 fungal genera were *Epicoccum* (D.O. Ribeiro), an unknown genus within the Pleospareaceae
351 family (D.O. Rías Baixas), and *Cyanodermella* (D.O. Valdeorras).

352
353 *3.5. The natural infection rates caused by fungal trunk pathogens differ between pruning times*
354

355 Among the identified taxa, 10 genera are generally regarded as being associated with GTDs:
356 *Botryosphaeria*, *Cadophora*, *Cryptovalsa*, *Cytospora*, *Diaporthe*, *Diplodia*, *Eutypa*,
357 *Neofusicoccum*, *Phaeoacremonium* and *Phaeomoniella*. Alpha-diversity of fungal
358 communities associated with GTDs in grapevine wood samples did not differ significantly
359 among D.O. (Chao1: $P = 0.1328$, Shannon: $P = 0.7608$; Fig. S7). The infection periods
360 predicted the summary metrics of alpha-diversities in D.O. Ribeiro (Chao1: $P = 0.041$,
361 Shannon: $P < 0.001$) and D.O. Rías Baixas (Chao1: $P < 0.001$, Shannon: $P < 0.001$), richness and
362 diversity being higher in the infection period 2 (Fig. 8a and 8b). The alpha-diversity of fungal
363 GTD communities did not differ between infection periods in D.O. Valdeorras ($P > 0.05$; Fig.
364 7c).

365 In the annual shoot (November: initial fungal microbiome), the percentages of fungal GTD
366 abundances with respect to the total fungal microbiome ranged from 0.1 to 0.7% (Fig. S8).
367 Regarding the infection periods, the percentages of fungal GTD abundances with respect to the
368 total fungal microbiome ranged from 0.2 to 1.2% (infection period 1) and from 0.3 to 1.9%
369 (infection period 2) (Fig. 9). The abundances of several fungal GTD genera increased
370 significantly in the infection period 2 compared to the infection period 1 ($P < 0.05$; Fig. 9):
371 *Cadophora* and *Diplodia* in D.O. Ribeiro, *Cadophora*, *Cytospora*, *Diaporthe*, *Diplodia*, *Eutypa*
372 and *Nefosicoccum* in D.O. Rías Baixas, and *Diaporthe* and *Phaeomoniella* in D.O. Valdeorras.
373 The abundance of *Cadophora* increased significantly in the infection period 1 compared to the
374 infection period 2 in D.O. Valdeorras ($P < 0.05$; Fig. 9c).

375
376 *3.6 Correlation with weather variables*
377

378 Climate conditions in each D.O and experimental season infection period is shown in Table
379 S4. Climate variables varied between pruning seasons and locations. The mean values of
380 temperature were similar during the winter season in D.O. Valdeorras (2017/2018: 6.52 °C;
381 2018/2019: 7.04 °C) and D.O. Ribeiro (2017/2018: 6.79 °C; 2018/2019: 7.44 °C), while they
382 were around 3 degrees on average higher in D.O. Rías Baixas (2017/2018: 9.42 °C; 2018/2019:
383 10.22 °C). In general, temperature declined after November pruning reaching its yearly
384 minimum during the winter season (Table S4). Temperature increased steadily from February
385 pruning until May pruning. Accumulated rainfall was very stable after November pruning
386 (winter season) at both D.O. Valdeorras (2017/2018: 298.40; 2018/2019: 309.60) and D.O.
387 Ribeiro (2017/2018: 322.20 mm; 2018/2019: 294.40 mm), but it was around 100 mm on
388 average higher in D.O. Rías Baixas (2017/2018: 393.30 mm; 2018/2019: 439.10 mm). After
389 February pruning (spring season), this parameter increased in 2017/2018 but decreased in
390 2018/2019, at the three D.O. studied. In general, D.O. Rías Baixas averaged the highest rainfall
391 among the three D.O. The relative humidity was highly stable at three locations and seasons,
392 and as expected higher rates were recorded during winter.

393 A significant correlation between the main weather variables and the OTU abundances of
394 the total fungal microbiome, *Diaporthe* and *Phaeomoniella* was detected (Table 2). Average
395 daily temperature for the 8-week period after pruning was negatively correlated ($P < 0.05$) with
396 the OTU abundances of the total fungal microbiome. Accumulated rainfall over 8 and 11 weeks

397 positively correlated with the fungal microbiome abundances ($P<0.05$). Regarding GTD fungal
398 genera, a negative correlation with temperature ($P<0.05$) was observed for *Diaporthe* and
399 *Phaeomoniella* in the first week after pruning. Accumulated rainfall over 8 and 11 weeks
400 positively correlated with *Diaporthe* abundances ($P<0.05$) (Table 2).

401 402 **4. Discussion**

403
404 In this study, we characterized the fungal community composition that colonizes grapevine
405 pruning wounds at two pruning times in six vineyards belonging to three D.O. in Spain. The
406 fungal microbiome across the three D.O. was largely composed by Ascomycota, followed by
407 Basidiomycota. The predominant fungal phylum found in this work is consistent with the
408 results obtained in other studies that explored the grapevine vascular tissue by culture dependent
409 (González and Tello, 2011; Hofstetter et al., 2012; Pancher et al., 2012; Bruez et al., 2014,
410 2016, 2017; Dissanayake et al., 2018; Eichmeier et al., 2018; Kraus et al., 2019) or by HTAS
411 (Dissanayake et al., 2018; Eichmeier et al., 2018; Deyett and Rolshausen, 2019, 2020;
412 Martínez-Diz et al., 2019b) approaches. The core microbiome included the ubiquitous, fast-
413 growing fungi *Aureobasidium* (Dothioraceae), *Cladosporium* (Cladosporiaceae), *Neofabraea*
414 (Dermateaceae) and *Epicoccum* (Didymellaceae). This result is in line with recent studies
415 aiming to decipher the fungal microbiome that resides in the xylem vessels of healthy grapevine
416 branches in Germany (Kraus et al., 2019), and in the sap of grapevine under high Pierce's
417 disease pressure in California (Deyett and Rolshausen, 2019).

418 The results obtained in D.O. Rías Baixas showed a significant fraction of variation in fungal
419 diversity (both the alpha and beta-diversity) that could be attributed to the infection period. It
420 is interesting to note that fungal richness and diversity obtained in the infection period
421 November-February was high relative to the period February-May in all D.O. In Mediterranean
422 climates, drier and colder conditions usually occur after early pruning in mid-autumn, while
423 wetter and warmer conditions favourable for fungal growth and infection occur progressively
424 after pruning in late winter (Luque et al., 2014). The lack of significant trend in fungal
425 microbiome abundances in both infection periods for all D.O. can be attributed to the Oceanic
426 climate conditions in Galicia region, with temperate and rainy periods from autumn to spring,
427 which may have favoured fungal spread and infection. In addition, two factors could also
428 contribute to the high abundance of microbial infection during November-February, namely the
429 wound healing and the bleeding processes. The wound healing involves the drying of the cane
430 tissues below the pruning wounds (Bostock and Stermer, 1989), which results in a dead wood
431 area called the drying cone (Lafon, 1921). In late winter and early spring, environmental
432 conditions are favourable for a rapid wound healing. When the weather is cold, pruning wounds
433 heal slowly leaving them open to fungal infection. In addition, bleeding of sap from the cut
434 ends of canes or spurs is the first sign of renewed activity. Bleeding alone might provide some
435 wound protection by flushing away fungal spores in early spring.

436 Spores are usually spread from sexual or asexual structures by wind, rain droplets or
437 arthropods, until they land on freshly and susceptible pruning wounds and with conditions of
438 optimal air temperature and moisture begin to germinate (Bettiga, 2013). In this study, the
439 correlation coefficients calculated between the mean daily temperature or the accumulated
440 rainfall and fungal microbiome infections showed negative values for temperature until eight
441 week after pruning, and positive and statistically significant correlations for rainfall at 8 and 11
442 weeks after pruning. An explanatory hypothesis for the negative correlations with temperature
443 variable might be related with a combination of favourable climatic conditions promoting a
444 faster and suitable pruning wound healing, which physically impeded the entrance of fungal
445 spores into the grapevine vascular tissue. Pruning grapevines in dry and warm weather is known
446 to enhance the mechanisms which reduce pruning wounds susceptibility (Munkvold and

447 Marois, 1995; Rolshausen et al., 2010). However, further research is required to confirm this
448 hypothesis. Positive correlations with accumulated rainfall could indicate that rain events have
449 an effect in increasing fungal microbiome abundance, and hence, pruning wounds infections.
450 Several studies found that spore release and airborne inoculum spread of fungal trunk pathogens
451 in vineyards coincided with the beginning and/or after periods of rain or irrigation events
452 (Pearson, 1980; Carter, 1991; Michailides and Morgan, 1993; Eskalen and Gubler, 2001;
453 Gubler et al., 2005; Amponsah et al., 2009; Kuntzmann et al., 2009; Trouillas and Gubler, 2009;
454 Úrbez-Torres et al., 2010a; van Niekerk et al., 2010; Baskarathevan et al., 2013; Gubler et al.,
455 2013; Úrbez-Torres et al., 2019). It has also been reported that rain can likely contribute to
456 pycnidia and conidia masses development (Anco et al., 2013; Onesti et al., 2017), and to the
457 splash-dispersal of conidia from pycnidia (González-Domínguez et al., 2020).

458 The linear discriminant analysis effect size detected several fungal clades, which
459 discriminated the fungal communities between infection periods. The fungal genus
460 *Aureobasidium* was predominant during the period November-February. Species of this genus,
461 in particular *A. pullulans*, is known to dominate the microbial consortia of grapevine (Sabate et
462 al., 2002; Martini et al., 2009; González and Tello, 2011; Barata et al., 2012; Pinto et al., 2014;
463 Dissanayake et al., 2018; Deyett and Rolshausen, 2019; Martínez-Diz et al., 2019b). *A.*
464 *pullulans* has evidenced great capacity to colonize grapevine pruning wounds (Munkvold and
465 Marois, 1993) and to act as a biocontrol agent of several grapevine post-harvest diseases
466 (Schena et al., 2002; Martini et al., 2009). This yeast-like fungus also showed antagonistic
467 abilities against *Eutypa lata*, the main causal agent of Eutypa dieback of grapevine, reducing of
468 up to 50% fungal infection in pruning wounds (Munkvold and Marois, 1993). In a recent study,
469 *A. pullulans* reduced the *in vitro* mycelial growth of *Diplodia seriata*, one of the causal agents
470 of Botryosphaeria dieback of grapevine, but no significant reduction of necrotic lesions were
471 found in grapevine cuttings (Pinto et al., 2018).

472 Several fungal genera associated with GTDs, such as *Cadophora*, *Cytospora*, *Diaporthe*,
473 *Diplodia* and *Phaeomoniella*, were mostly identified during the infection period February-May
474 and explained the differences observed between periods. Cross-infection throughout both
475 periods was unlikely to occur given the long wood section of approximately 15-cm left between
476 sampling periods. Using artificial inoculations with extreme disease pressure, the farthest
477 downward growth for a fast-growing fungus such as *E. lata* was estimated to be 4 cm at 5
478 months after inoculation (Weber et al., 2007), and the overall mean of the GTD pathogens *D.*
479 *seriata* and *Phaeomoniella chlamydospora* recovery five months after inoculation were 54.2%
480 and 46.9%, respectively, at 4.5 cm below the pruning wound (Elena and Luque, 2016).
481 Noticeably, low GTD fungal abundance were detected in annual shoots. The data support the
482 evidence that these fungi prefer perennial woody stems, which is where wood symptoms
483 associated with GTDs are commonly found (Gramaje et al., 2018).

484 Trunk disease fungi are mainly spread through aerially dispersed spores infecting
485 grapevines via pruning and/or natural wounds (Rolshausen et al., 2010; van Niekerk et al., 2011;
486 Gramaje et al., 2018). Spore release varies throughout the growing season depending on the
487 fungal pathogen, geographical location and environmental conditions (Larignon and Dubos,
488 2000; Eskalen and Gubler, 2001; Quaglia et al., 2009; Úrbez-Torres et al. 2010a, 2010b; van
489 Niekerk et al., 2010; Billones-Baaijens et al., 2018; González-Domínguez et al., 2020), so
490 information related to the dispersal patterns of GTD pathogens are indispensable to identify
491 high-risk infection periods and to guide growers in timing management practices such as
492 pruning time. In this sense, González-Domínguez et al. (2020) recently developed a model to
493 predict disease risk caused by *Pa. chlamydospora* in vineyards and estimated that the pathogen
494 dynamics were best explained when time was expressed as hydro-thermal time accounting for
495 the effects of both temperature and rain. In the present study, evolution patterns of the
496 correlation coefficients between weather data and OTUs abundance of GTD pathogens have

497 been irregular with negatively and positively values being rarely statistically significant. In the
498 first week after pruning, temperature was negatively correlated with *Diaporthe* and
499 *Phaeomoniella* genus abundances and as previously discussed for the fungal microbiome, this
500 fact could be associated with a mixture of proper climatic conditions favouring the pruning
501 wound healing process. Negative correlations values between mean daily temperature and *D.*
502 *seriata* and *Pa. chlamydospora* natural infections were also found in the first weeks after
503 pruning by Luque et al. (2014). Accumulated rainfall was found to have a positive significant
504 correlation with *Diaporthe* from eight weeks highlighting again the role of rain events in the
505 infection and development of GTDs fungal pathogens, as earlier considered for the fungal
506 microbiome. This same trend was also observed by Luque et al. (2014) for natural infections
507 caused by *D. seriata*, *Pa. chlamydospora* and species of Diatrypaceae in Catalanian vineyards.

508 Susceptibility of grapevine pruning wounds to trunk pathogens have been studied through
509 artificial fungal inoculations in several grape-growing regions such as Australia (Ayres et al.,
510 2016), California (Moller and Kasimatis, 1978; Munkvold and Marois, 1995; Eskalen et al.,
511 2007; Úrbez-Torres and Gubler, 2011), France (Chapuis et al., 1998; Larignon and Dubois,
512 2000; Lecomte and Bailey, 2011), Italy (Serra et al., 2008), Michigan (Trese et al., 1982), South
513 Africa (van Niekerk et al., 2011) and Spain (Elena and Luque, 2016). In general, these studies
514 showed that wound susceptibility decreased as the period between pruning and inoculation of
515 wounds increased, and it can be extended up to four to seven weeks for most pathogens under
516 favourable conditions. The rate of natural infections in pruned canes (i.e., those not obtained
517 through artificial inoculations), however, has not been extensively studied to date, and they can
518 be estimated only through the spontaneous infections of the vines included as non-inoculated
519 controls in artificial inoculations.

520 Results obtained in our study on the natural infections of pruning wounds in three D.O. in
521 Galicia showed that higher fungal GTD infection abundances occurred more frequently in
522 spring than in winter, thus suggesting that pruning wounds could be more susceptible to
523 pathogens overall after a late pruning in winter. Similar results were obtained by Luque et al.
524 (2014), who observed higher isolation percentages of several GTD fungi in culture medium
525 following late pruning (February-May) compared with that following early pruning
526 (November-February). In contrast, mean percentage values of natural infections caused by
527 *Eutypa lata* were about 2% after the spring-pruning (mid-May to late June) and 13% after the
528 winter pruning (January to February) in France (Lecomte and Bailey, 2011). Studies based on
529 artificial inoculations also recommended late pruning to reduce GTD pathogens infections
530 (Petzoldt et al., 1981; Munkvold and Marois, 1995; Chapuis et al., 1998; Larignon and Dubois,
531 2000; Eskalen et al., 2007; Serra et al., 2008, Úrbez-Torres and Gubler, 2011), although the real
532 potential risk of infections may have been biased since these trials did not consider the presence
533 of natural pathogenic inoculum along the experimental period.

534 In conclusion, a broad range of fungi was able to colonize grapevine pruning wounds at
535 both infection periods. Pruned canes harbour a core community of fungal species, which appear
536 to be independent of the infection period. In light of the GTD colonization results and given the
537 environmental conditions and the geographical location of this study, early pruning is
538 recommended to reduce the infections caused by GTD fungi during the pruning season in
539 Galicia. It is important to note that read counts in HTAS approach are considered as semi-
540 quantitative (Amend et al., 2010). This means that there is no real quantitative relationship
541 between spore count and read count, although a significant correlation between sequencing
542 reads and the relative abundance of DNA of GTD fungi have been recently observed in soil
543 samples (Berlanas et al., 2019). If precise indication of aerial spore load for one specific fungal
544 species is required, quantitative PCR would become the tool of choice. In this sense, high-
545 throughput droplet digital PCR protocols have been recently developed for absolute

546 quantification of GTD fungi from environmental samples (Holland et al., 2019; Maldonado-
547 González et al., 2020; Martínez-Diz et al., 2020).

548

549 **Acknowledgments**

550 Funding was provided by Ministerstvo Školství, Mládeže a Tělovýchovy
551 (CZ.02.1.01./0.0/0.0/16_017/0002334).

552

553 **References**

- 554 Aigoun-Mouhous, W., Elena, G., Cabral, A., León, M., Sabaou, N., Armengol, J., 2019.
555 Characterization and pathogenicity of *Cylindrocarpon*-like asexual morphs associated
556 with black foot disease in Algerian grapevine nurseries, with the description of
557 *Pleioicarpion algeriense* sp. nov. Eur. J. Plant Pathol. 154, 887-901.
- 558 Amend, S.A., Seifert, K.A., Bruns, T.D., 2010. Quantifying microbial communities with 454
559 pyrosequencing: does read abundance count? Mol. Ecol. 19, 5555-5565.
- 560 Amann, R.L., Ludwig, W., Schleifer, K.H., 1995. Phylogenetic identification and in situ
561 detection of individual microbial cells without cultivation. Microbiol. Rev. 59, 143-169.
- 562 Amponsah, N.T., Jones, E.E., Ridgway, H.J., Jaspers, M.V., 2009. Rainwater dispersal of
563 Botryosphaeria conidia from infected grapevines. New Zealand Plant Prot. 62, 228-233.
- 564 Anco, D.J., Madden, L.V., Ellis, M.A., 2013. Effects of temperature and wetness duration on
565 the sporulation rate of *Phomopsis viticola* on infected grape canes. Plant Dis. 97, 579-589.
- 566 Andrews, S., 2010. FastQC: a quality control tool for high throughput sequence data. Available
567 online at: <http://www.bioinformatics.babraham.ac.uk/projects/fastqc>.
- 568 Ayres, M., Billones-Baaijens, R., Savocchia, S., Scott, E., Sosnowski, M., 2016. Susceptibility
569 of pruning wounds to grapevine trunk disease pathogens. Wine Vitic. J. 31, 48-50.
- 570 Baldan, E., Nigris, S., Populin, F., Zottini, M., Squartini, A., Baldan, B., 2014. Identification of
571 culturable bacterial endophyte community isolated from tissues of *Vitis vinifera* "Glera".
572 Plant Biosyst. 148, 508-516.
- 573 Barata, A., Malfeito-Ferreira, M., Loureiro, V., 2012. The microbial ecology of wine grape
574 berries. Int. J. Food Microbiol. 153, 243-259.
- 575 Baskarathevan, J., Jaspers, M.V., Jones, E.E., Ridgway, H.J., 2013. Development of isolate-
576 specific markers for *Neofusicoccum parvum* and *N. luteum* and their use to study rainwater
577 splash dispersal in the vineyard. Plant Pathol. 62, 501-509.
- 578 Bettiga, L.J., 2013. Grape Pest Management, University of California, Agriculture and Natural
579 Resources, Publication 3343.
- 580 Berlanas, C., Berbegal, M., Elena, G., Laidani, M., Cibriain, J.F., Sagües, A., Gramaje, D.,
581 2019. The fungal and bacterial rhizosphere microbiome associated with grapevine
582 rootstock genotypes in mature and young vineyards. Frontiers Microbiol. 10, 1142.
- 583 Berlanas, C., Ojeda, S., López-Manzanares, B., Andrés-Sodupe, B., Bujanda, R., Martínez-Diz,
584 M.P., Díaz-Losada, E., Gramaje, D., 2020. Occurrence and diversity of black-foot disease
585 fungi in symptomless grapevine nursery stock in Spain. Plant Dis. 104, 94-104. doi:
586 10.1094/PDIS-03-19-0484-RE
- 587 Billones-Baaijens, R., Úrbez-Torres, J.R., Liu, M., Ayres, M., Sosnowski, M., Savocchia, S.,
588 2018. Molecular methods to detect and quantify Botryosphaeriaceae inocula associated
589 with grapevine dieback in Australia. Plant Dis. 102, 1489-1499.
- 590 Bostock, R.M., Stermer, B.A., 1989. Perspectives on wound healing in resistance to pathogens.
591 Annu. Rev. Phytopathol. 27, 343-371.
- 592 Brown, A.A., Lawrence, D.P., Baumgartner, K., 2020. Role of basidiomycete fungi in the
593 grapevine trunk disease esca. Plant Pathol. <https://doi.org/10.1111/ppa.13116>.
- 594 Bruez, E., Vallance, J., Gerbore, J., Lecomte, P., Da Costa, J. P., Guerin-Dubrana, L., Rey, P.,
595 2014. Analyses of the temporal dynamics of fungal communities colonizing the healthy

- 596 wood tissues of esca leaf-symptomatic and asymptomatic vines. PLoS ONE 9, e95928.
597 Bruez, E., Baumgartner, K., Bastien, S., Travadon, R., Guérin-Dubrana, L., Rey, P., 2016.
598 Various fungal communities colonise the functional wood tissues of old grapevines
599 externally free from grapevine trunk disease symptoms. Aust. J. Grape Wine Res. 22, 288-
600 295.
- 601 Bruez, E., Larignon, P., Compant, S., Rey, P., 2017. Investigating the durable effect of the hot
602 water treatment used in nurseries on pathogenic fungi inhabiting grapevine wood and
603 involved in Grapevine Trunk Diseases. Crop Protect. 100, 203-210.
- 604 Carter, M.V., 1991. The status of *Eutypa lata* as a pathogen. Monogr. Phytopathol. Pap. No 32.
605 Commonwealth Agricultural Bureau, International Mycological Institute, Wallingford,
606 Oxfordshire, U.K.
- 607 Chapuis, L., Richard, L., Dubos, B., 1998. Variation in susceptibility of grapevine pruning
608 wound to infection by *Eutypa lata* in south-western France. Plant Pathol. 47, 463-72.
- 609 Cloete et al., 2015 Cloete, M., Fischer, M., Mostert, L., Halleen, F., 2015. Hymenochaetales
610 associated with esca-related wood rots on grapevine with a special emphasis on the status
611 of esca in South African vineyards. Phytopathol. Mediterr. 54, 299-312.
- 612 Compant, S., Mitter, B., Colli-Mull, J.G., Gangl, H., Sessitsch, A., 2011. Endophytes of
613 grapevine flowers, berries, and seeds: identification of cultivable bacteria, comparison
614 with other plant parts, and visualization of niches of colonization. Microb. Ecol. 62, 188-
615 197. doi: 10.1007/s00248-011-9883-y
- 616 Deyett, E., Roper, M.C., Ruegger, P., Yang, J., Borneman, J., Rolshausen, P.E., 2017. Microbial
617 landscape of the grapevine endosphere in the context of Pierce's disease. Phytobiomes 1,
618 138-149. doi: 10.1094/PBIOMES-08-17-0033-R
- 619 Deyett, E., Rolshausen, P.E., 2019. Temporal Dynamics of the Sap Microbiome of Grapevine
620 Under High Pierce's Disease Pressure. Front. Plant Sci. 10, 1246. doi:
621 10.3389/fpls.2019.01246
- 622 Deyett, E., Rolshausen, P.E., 2020. Endophytic Microbial Assemblage in Grapevine. FEMS
623 Microbiol. Ecol., fiae053. <https://doi.org/10.1093/femsec/fiae053>
- 624 Dhariwal, A., Chong, J., Habib, S., King, I. L., Agellon, L. B., Xia, J., 2017.
625 MicrobiomeAnalyst: A web-based tool for comprehensive statistical, visual and meta-
626 analysis of microbiome data. Nucleic Acids Res. 45, W180–W188.
627 doi:10.1093/nar/gkx295.
- 628 Dissanayake, A.J., Purahong, W., Wubet, T., Hyde, K.D., Zhang, W., Xu, H., Zhang, G., Fu,
629 F., Liu, M., Xing, Q., Li, X., Yan, J., 2018. Direct comparison of culture-dependent and
630 culture-independent molecular approaches reveal the diversity of fungal endophytic
631 communities in stems of grapevine (*Vitis vinifera*). Fungal Divers. 90, 85-107.
- 632 Eichmeier, A., Pecenka, J., Penázová, E., Baránek, M., Català-García, S., León, M., Armengol,
633 J., Gramaje, D., 2018. High-throughput amplicon sequencing-based analysis of active
634 fungal communities inhabiting grapevine after hot-water treatments reveals unexpectedly
635 high fungal diversity. Fungal Ecol. 36, 26-38.
636 <https://doi.org/10.1016/j.funeco.2018.07.011>
- 637 Eskalen, A., Gubler, W.D., 2001. Association of spores of *Phaeoconiella chlamydospora*,
638 *Phaeoacremonium inflatipes*, and *Pm. aleophilum* with grapevine cordons in California.
639 Phytopathol. Mediterr. 40S, 429-432.
- 640 Eskalen, A., Feliciano, J., Gubler, W.D., 2007. Susceptibility of grapevine pruning wounds and
641 symptom development in response to infection by *Phaeoacremonium aleophilum* and
642 *Phaeoconiella chlamydospora*. Plant Dis. 91, 1100-1104.
- 643 Elena, G., Luque, J., 2016. Seasonal susceptibility of pruning wounds and cane colonization in
644 Catalonia, Spain following artificial infection with *Diplodia seriata* and *Phaeoconiella*
645 *chlamydospora*. Plant Dis. 100, 1651-1659.

- 646 Faist, H., Keller, A., Hentschel, U., Deeken, R., 2016. Grapevine (*Vitis vinifera*) crown galls
647 host distinct microbiota. *Appl. Environ. Microb.* 82, 5542-5552.
- 648 Fischer, M., 2002. A new wood-decaying basidiomycete species associated with esca of
649 grapevine: *Fomitiporia mediterranea* (Hymenochaetales). *Mycol. Prog.* 1, 315-324.
- 650 Glynou, K., Nam, B., Thines, M., Maciá-Vicente, J.G., 2018. Facultative root-colonizing fungi
651 dominate endophytic assemblages in roots of nonmycorrhizal *Microthlaspsi* species. *New*
652 *Phytol.* 217, 1190-1202.
- 653 Gramaje, D., Úrbez-Torres, J.R., Sosnowski, M.R., 2018. Managing grapevine trunk diseases
654 with respects to etiology and epidemiology: current strategies and future prospects. *Plant*
655 *Dis.* 102, 12-39.
- 656 González, M., Tello, M., 2011. The endophytic mycota associated with *Vitis vinifera* in central
657 Spain. *Fungal Divers.* 47, 29-42.
- 658 González-Domínguez, E., Berlanas, C., Gramaje, D., Armengol, J., Rossi, V., Berbegal, M.,
659 2020. Temporal dispersal patterns of *Phaeomoniella chlamydospora*, causal agent of Petri
660 disease and esca, in vineyards. *Phytopathology*. [https://doi.org/10.1094/PHYTO-10-19-](https://doi.org/10.1094/PHYTO-10-19-0400-R)
661 [0400-R](https://doi.org/10.1094/PHYTO-10-19-0400-R)
- 662 Gubler, W.D., Rolshausen, P.E., Trouillas, F.P., Úrbez-Torres, J.R., Voegel, T., Leavitt, G. M.,
663 Weber, E.A., 2005. Grapevine trunk diseases in California. *Practical Winery Vineyard*
664 January-February, 6-25.
- 665 Gubler, W.D., Rooney-Latham, S., Vasquez, S.J., Eskalen, A., 2013. Esca (Black Measles) and
666 Petri disease, in: Bettiga, L.J. (Ed.), *Grape Pest Management*, University of California,
667 Agriculture and Natural Resources, Publication 3343.
- 668 Hofstetter, V., Buyck, V., Croll, D., Viret, O., Couloux, A., Gindro, K. 2012. What if esca
669 disease of grapevine were not a fungal disease?. *Fungal Divers.* 54, 51-67.
- 670 Holland, T., Bowen, P., Kokkoris, V., Úrbez-Torres, J.R., Hart, M. 2019. Does inoculation with
671 arbuscular mycorrhizal fungi reduce trunk disease in grapevine rootstocks?. *Horticulturae*
672 5, 61.
- 673 Jackson, R.S., 2004. *Wine Science: Principles and Applications*. Academic Press. 978 pp.
- 674 Kraus, C., Voegele, R.T., Fischer, M., 2019. Temporal Development of the Culturable,
675 Endophytic Fungal Community in Healthy Grapevine Branches and Occurrence of GTD-
676 Associated Fungi. *Microb. Ecol.* 77, 866–876.
- 677 Kuntzmann, P., Villaume, S., Bertsch, C., 2009. Conidia dispersal of *Diplodia* species in a
678 French vineyard. *Phytopathol. Mediterr.* 48, 150-154.
- 679 Lafon R., 1921. L'apoplexie: traitement préventif (Méthode Poussard), traitement curative, in:
680 Modifications à Apporter à la Taille de la Vigne dans les Charentes: taille Guyot-Poussard
681 Mixte et Double, Imprimerie Roumégous et Déhan, Montpellier, France, pp. 35-44.
- 682 Larignon, P., Dubos, B., 2000. Preliminary studies on the biology of *Phaeoacremonium*.
683 *Phytopathol. Mediterr.* 39, 184-189.
- 684 Lawrence, D.P., Nouri, M.T., Trouillas, F.P., 2019. Taxonomy and multi-locus phylogeny of
685 *Cylindrocarpon*-like species associated with diseased roots of grapevine and other fruit
686 and nut crops in California. *Fungal Syst. Evol.* 4, 59-75.
- 687 Lawrence, D.P., Travadon, R., Pouzoulet, J., Rolshausen, P.E., Wilcox, W.F., Baumgartner,
688 K., 2017. Characterization of *Cytospora* isolates from wood cankers of declining grapevine
689 in North America, with the descriptions of two new *Cytospora* species. *Plant Pathol.* 66,
690 713-725.
- 691 Lecomte, P., Bailey, D.J., 2011. Studies on the infestation by *Eutypa lata* of grapevine spring
692 wounds. *Vitis* 50, 35-41.
- 693 Luque, J., Elena, G., Garcia-Figueroles, F., Reyes, J., Barrios, G., Legorburu, F.J., 2014. Natural
694 infections of pruning wounds by fungal trunk pathogens in mature grapevines in Catalonia
695 (Northeast Spain). *Aust. J. Grape Wine Res.* 20, 134-143.

- 696 Makatini, G., Mutawila, C., Halleen, F., Mostert, L., 2014. Grapevine sucker wounds as
697 infection ports for trunk disease pathogens. *Phytopathol. Mediterr.* 53, 573.
- 698 Maldonado-González, M.M., Martínez-Diz, M.P., Andrés-Sodupe, M., Bujanda, R., Díaz-
699 Losada, E., Gramaje, D., 2020. Quantification of *Cadophora luteo-olivacea* from
700 grapevine nursery stock and vineyard soil using droplet digital PCR. *Plant Dis.*
701 <https://doi.org/10.1094/PDIS-09-19-2035-RE>
- 702 Martínez-Diz, M.P., Andrés-Sodupe, M., Bujanda, R., Díaz-Losada, E., Eichmeier, A.,
703 Gramaje, D., 2019b. Soil-plant compartments affect fungal microbiome diversity and
704 composition in grapevine. *Fungal Ecol.* 41, 234-244.
- 705 Martínez-Diz, M.P., Díaz-Losada, E., Barajas, E., Ruano-Rosa, D., Andrés-Sodupe, M.,
706 Gramaje, D., 2019a. Screening of Spanish *Vitis vinifera* germplasm for resistance to
707 *Phaeomoniella chlamydospora*. *Sci. Hortic.* 246, 104-109.
- 708 Martínez-Diz, M.P., Andrés-Sodupe, M., Berbegal, M., Bujanda, R., Díaz-Losada, E., Gramaje,
709 D., 2020. Droplet Digital PCR Technology for Detection of *Ilyonectria liriodendri* from
710 Grapevine Environmental Samples. *Plant Dis.* 104, 1144-1150.
711 <https://doi.org/10.1094/PDIS-03-19-0529-RE>
- 712 Martini, M., Musetti, R., Grisan, R., Polizzotto, R., Borselli, S., Pavan, F., Osler, R., 2009.
713 DNA-dependent detection of the grapevine fungal endophytes *Aureobasidium pullulans*
714 and *Epicoccumnigrum*. *Plant Dis.* 93, 993-998.
- 715 Michailides, T.J., Morgan, D.P., 1993. Spore release by *Botryosphaeria dothidea* in pistachio
716 orchards and disease control by altering the trajectory angle of sprinklers. *Phytopathology*
717 83, 145-152.
- 718 Moller, W.S., Kasimatis, A.N., 1978. Dieback of grapevines caused by *Eutypa armeniaceae*.
719 *Plant Dis. Rep.* 62, 254-258.
- 720 Moller, W. J., Kasimatis, J., 1980. Protection of grapevine pruning wounds from *Eutypa*
721 dieback. *Plant Dis.* 64, 278-280.
- 722 Munkvold, G.P., Marois, J.J., 1993. Efficacy of natural epiphytes and colonisers of grapevine
723 pruning wounds for biological control of *Eutypa* dieback. *Phytopathology* 83, 624-629.
- 724 Munkvold, G.P., Marois, J.J., 1995. Factors associated with variation in susceptibility of
725 grapevine pruning wounds to infection by *Eutypa lata*. *Phytopathology* 85, 249-256.
- 726 Nguyen, N.H., Smith, D., Peay, K., Kennedy, P., 2015. Parsing ecological signal from noise in
727 next generation amplicon sequencing. *New Phytol.* 205, 1389-1393.
- 728 Onesti, G., González-Domínguez, E., Rossi, V., 2017. Production of pycnidia and conidia by
729 *Guignardia bidwellii*, the causal agent of grape black rot, as affected by temperature and
730 humidity. *Phytopathology* 107, 173-183.
- 731 Pancher, M., Ceol, M., Corneo, P.E., Longa, C.M.O., Yousaf, S., Pertot, I., Campisano, A.,
732 2012. Fungal endophytic communities in grapevines (*Vitis vinifera* L.) respond to crop
733 management. *Appl. Environ. Microbiol.* 78, 4308-4317.
- 734 Pearson, R.C., 1980. Discharge of ascospores of *Eutypa armeniaceae* in New York. *Plant Dis.*
735 64, 171-174.
- 736 Petzoldt, C.H., Moller, W.J., Sall, M.A., 1981. *Eutypa* dieback of grapevines: seasonal
737 differences in infection and duration of susceptibility of pruning wounds. *Phytopathology*
738 71, 540-543.
- 739 Petzoldt, C. H., Sall, M. A., Moller, W. J., 1983. *Eutypa* Dieback of Grapevines: Ascospore
740 Dispersal in California *Am. J. Enol. Vitic.* 34, 265-270.
- 741 Perazzolli, M., Antonielli, L., Storari, M., Puopolo, G., Pancher, M., Giovannini, O., Pindo, M.,
742 Pertot, I., 2014. Resilience of the natural phyllosphere microbiota of the grapevine to
743 chemical and biological pesticides. *Appl. Environ. Microb.* 80, 3585-3596.
- 744 Pinto, C., Pinho, D., Sousa, S., Pinheiro, M., Egas, C., Gomes, A.C., 2014. Unravelling the
745 diversity of grapevine microbiome. *PLoS One* 9:e85622.

- 746 Pinto, C., dos Santos Custódio, V., Nunes, M, Songy, A., Rabenoelina, F., Courteaux, B.,
747 Clément, C., Catarina-Gomes, A., Fontaine, F., 2018. Understand the potential role of
748 *Aureobasidium pullulans*, a resident microorganism from grapevine, to prevent the
749 infection caused by *Diplodia seriata*. Front Microbiol. 9, 3047. doi:
750 10.3389/fmicb.2018.03047.
- 751 Quaglia, M., Covarelli, L., Zazzerini, A., 2009. Epidemiological survey on esca disease in
752 Umbria, central Italy. Phytopathol. Mediterr. 48, 84-91.
- 753 R Core Team, 2019. R: A language and environment for statistical computing. R Foundation
754 for Statistical Computing, Vienna, Austria. <http://www.r-project.org/index.html>
- 755 Rolshausen, P.E., Úrbez-Torres, J.R., Rooney-Latham, S., Eskalen, A., Smith, R.J., Gubler
756 W.D., 2010. Evaluation of pruning wound susceptibility and protection against fungi
757 associated with grapevine trunk diseases. Am. J. Enol. Vitic. 61, 113-119.
- 758 Sabate, J., Cano, J., Esteve-Zarzoso, B., Guillamón, J.M., 2002. Isolation and identification of
759 yeasts associated with vineyard and winery by RFLP analysis of ribosomal genes and
760 mitochondrial DNA. Microbiol. Res. 157, 267-274.
- 761 Schena, L., Sialer, M. F., Gallitelli, D., 2002. Molecular detection of strain L47 of
762 *Aureobasidium pullulans*, a biocontrol agent of postharvest diseases. Plant Dis. 86, 54-60.
- 763 Segata, N., Izard, J., Waldron, L., Gevers, D., Miropolsky, L., Garrett, W. S., Huttenhower, C.,
764 2011. Metagenomic biomarker discovery and explanation. Genome Biol. 12, R60.
765 doi:10.1186/gb-2011-12-6-r60.
- 766 Serra, S., Mannoni, A.M., Ligios, V., 2008. Studies on the susceptibility of pruning wounds to
767 infection by fungi involved in grapevine wood diseases in Italy. Phytopathol. Mediterr.
768 47, 234-246.
- 769 Studholme, D.J., Glover, R.H., Boonham, N., 2011. Application of high-throughput DNA
770 sequencing in phytopathology. Annu. Rev. Phytopathol. 49, 87-105.
- 771 Trese, A.T., Ramsdell, C.D., Burton, C.L., 1982. Effects of winter and spring pruning and
772 postinoculation cold weather on infection of grapevine by *Eutypa armeniacae*.
773 Phytopathology 72, 438-440.
- 774 Trouillas, F.P., 2009. Taxonomy and biology of *Eutypa* and other diatrypaeceae species
775 associated with grapevine canker diseases in California. Ph.D. dissertation, University of
776 California, Davis.
- 777 Trouillas, F.P., Gubler, W.D., 2009. The status of *Eutypa lata* in California. Phytopathol.
778 Mediterr. 48, 161-162.
- 779 Turenne, C.Y., Sanche, S.E., Hoban, D.J., Karlowsky, J.A., Kabani, A.M., 1999. Rapid
780 identification of fungi by using the ITS2 genetic region and an automated fluorescent
781 capillary electrophoresis system. J. Clin. Microbiol. 37, 1846-1851.
- 782 Úrbez-Torres, J.R., Battany, M., Bettiga, L.J., Gispert, C., McGourty, G., Roncoroni, J., Smith,
783 R.J., Verdegaal, P., Gubler, W.D., 2010a. Botryosphaeriaceae species spore-trapping
784 studies in California Vineyards. Plant Dis. 94, 717-724.
- 785 Úrbez-Torres, J.R., Bruez, E., Hurtado, J., Gubler, W.D., 2010b. Effect of temperature on
786 conidial germination of Botryosphaeriaceae species infecting grapevines. Plant Dis. 94,
787 1476-1484.
- 788 Úrbez-Torres, J.R., Gubler, W.D. 2011. Susceptibility of grapevine pruning wounds to infection
789 by *Lasiodiplodia theobromae* and *Neofusicoccum parvum*. Plant Pathol. 60, 261-270.
- 790 Úrbez-Torres, J.R., Gispert, C., Trouillas, F.P., 2019. Epidemiology of Diatrypaeceae spp. in
791 California vineyards. Phytopathol. Mediterr. 58, 449.
- 792 van Niekerk, J.M., Calitz, F.J., Halleen, F., Fourie, P.H., 2010. Temporal spore dispersal
793 patterns of grapevine trunk pathogens in South Africa. Eur. J. Plant. Pathol. 127, 375-390.
- 794 van Niekerk, J.M., Calitz, F.J., Halleen, F., Fourie, P.H., 2011. Temporal susceptibility of
795 grapevine pruning wounds to trunk pathogen infection in South African grapevines.

- 796 Phytopathol. Mediterr. 50, S139-S150.
- 797 Valencia, D., Torres, C., Camps, R., Lopez, E., Celis-Diez, J., Beosain, X., 2015. Dissemination
798 of Botryosphaeriaceae conidia in vineyards in the semiarid Mediterranean climate of the
799 Valparaíso Region of Chile. Phytopathol. Mediterr. 54, 394-402.
- 800 Vázquez-Baeza, Y., Pirrung, M., Gonzalez, A., Knight, R., 2013. EMPeror: A tool for
801 visualizing high-throughput microbial community data. Gigascience 2. doi:10.1186/2047-
802 217X-2-16.
- 803 Weber, E.A., Trouillas, F.P., Gubler, W.D., 2007. Double pruning of grapevines: A cultural
804 practice to reduce infections by *Eutypa lata*. Am. J. Enol. Vitic. 58, 61-66.
- 805 West, E.R., Cother, E.J., Steel, C.C., Ash, G.J., 2010. The characterization and diversity of
806 bacterial endophytes of grapevine. Can. J. Microbiol. 56, 209-216.
- 807 White, T. J., Bruns, T., Lee, S. H., Taylor, J. W., 1990. Amplification and direct sequencing of
808 fungal ribosomal RNA genes for phylogenetics, in: Innis, M.A., Gelfand, D.H., Sninsky,
809 J.J., White, T.J. (Eds.), PCR Protocols: A Guide to Methods and Applications, Academic
810 Press, San Diego, CA, pp. 315–322.
- 811 Zarraonaindia, I., Owens, S.M., Weisenhorn, P., West, K., Hampton-Marcell, J., Lax, S.,
812 Bokulich, N.A., Mills, D.A., Martin, G., Taghavi, S., van der Lelie, D., Gilbert, J.A., 2015.
813 The soil microbiome influences grapevine-associated microbiota. MBio 6.
814 doi:10.1128/mBio.02527-14.
- 815 Zheng, W., García, J., Balda, P., Martínez de Toda, F., 2017. Effects of late Winter pruning at
816 different phenological stages on vine yield components and berry composition in La Rioja,
817 North-central Spain. OENO One 51, 363-372.

Table 1

Experimental factors predicting alpha-diversity of pruning wounds associated fungal communities in three Denomination of Origin (D.O.) in Galicia.

	D.O. Ribeiro		D.O. Rías Baixas		D.O. Valdeorras	
	Shannon	Chao1	Shannon	Chao1	Shannon	Chao1
Year	$F = 3.01$ $P = 0.9129$	$F = 2.99$ $P = 0.6998$	$F = 2.99$ $P = 0.4553$	$F = 2.79$ $P = 0.211$	$F = 4.55$ $P = 0.1552$	$F = 4.22$ $P = 0.4761$
Experimental plot	$F = 2.13$ $P = 0.1455$	$F = 1.26$ $P = 0.0647$	$F = 3.05$ $P = 0.3550$	$F = 3.77$ $P = 0.1295$	$F = 3.12$ $P = 0.6772$	$F = 3.79$ $P = 0.8890$
Year x experimental plot	$F = 0.85$ $P = 0.8773$	$F = 0.95$ $P = 0.4103$	$F = 1.14$ $P = 0.1445$	$F = 1.92$ $P = 0.2301$	$F = 2.99$ $P = 0.9778$	$F = 3.76$ $P = 0.9110$
Infection period*	$F = 4.21$ $P = 0.7468$	$F = 3.72$ $P = 0.0416$	$F = 3.75$ $P < 0.001$	$F = 5.06$ $P < 0.001$	$F = 4.25$ $P = 0.9079$	$F = 4.20$ $P = 0.1221$
Year x infection period	$F = 1.83$ $P = 0.2340$	$F = 0.90$ $P = 0.0981$	$F = 2.19$ $P = 0.1221$	$F = 4.26$ $P = 0.2543$	$F = 2.35$ $P = 0.4551$	$F = 1.88$ $P = 0.2989$
Experimental plot x infection period	$F = 3.24$ $P = 0.1134$	$F = 4.01$ $P = 0.0944$	$F = 3.11$ $P = 0.0987$	$F = 5.79$ $P = 0.1556$	$F = 5.67$ $P = 0.2375$	$F = 4.15$ $P = 0.6780$

*Infection period: 1 (from November to February) and 2 (from February to May)

Table 2

Spearman's correlation coefficients of the relationships between weather data and OTUs number of the total fungal microbiome, *Cadophora*, *Diaporthe*, *Diplodia*, *Phaeoacremonium* and *Phaeomoniella*. All OTU data are log transformed.

Correlation coefficient and significance	Fungal microbiome			<i>Cadophora</i>			<i>Diaporthe</i>			<i>Diplodia</i>			<i>Phaeoacremonium</i>			<i>Phaeomoniella</i>		
	T1*	RH1	LCR1	T1	RH1	LCR1	T1	RH1	LCR1	T1	RH1	LCR1	T1	RH1	LCR1	T1	RH1	LCR1
r	-0.938	0.143	0.306	-0.146	0.262	-0.067	-0.599	0.303	0.161	-0.380	0.303	0.161	-0.068	0.102	-0.298	-0.731	0.102	-0.298
P	<0.01	0.658	0.333	0.649	0.409	0.833	0.039	0.337	0.676	0.229	0.337	0.676	0.831	0.750	0.346	<0.01	0.750	0.346
	T2	RH2	LCR2	T2	RH2	LCR2	T2	RH2	LCR2	T2	RH2	LCR2	T2	RH2	LCR2	T2	RH2	LCR2
r	-0.754	0.103	-0.188	-0.148	0.251	-0.224	-0.372	0.265	-0.017	-0.212	0.254	-0.430	0.066	0.161	0.328	-0.382	-0.074	0.006
P	0.004	0.751	0.558	0.646	0.414	0.492	0.231	0.404	0.955	0.507	0.424	0.162	0.838	0.617	0.282	0.219	0.818	0.984
	T4	RH4	LCR4	T4	RH4	LCR4	T4	RH4	LCR4	T4	RH4	LCR4	T4	RH4	LCR4	T4	RH4	LCR4
r	-0.819	-0.048	0.494	-0.213	0.190	0.170	-0.436	0.022	0.522	-0.341	0.129	-0.303	0.071	0.027	0.014	-0.487	-0.242	0.268
P	<0.01	0.882	0.102	0.505	0.552	0.596	0.156	0.944	0.081	0.277	0.689	0.338	0.824	0.933	0.966	0.107	0.447	0.398
	T8	RH8	LCR8	T8	RH8	LCR8	T8	RH8	LCR8	T8	RH8	LCR8	T8	RH8	LCR8	T8	RH8	LCR8
r	-0.634	0.777	0.733	-0.092	0.070	0.166	-0.244	0.165	0.708	-0.197	0.127	0.447	0.137	-0.188	-0.002	-0.327	-0.160	0.481
P	0.027	0.580	0.006	0.775	0.827	0.605	0.443	0.608	<0.01	0.588	0.692	0.145	0.670	0.557	0.847	0.299	0.619	0.113
	T11	RH11	LCR11	T11	RH11	LCR11	T11	RH11	LCR11	T11	RH11	LCR11	T11	RH11	LCR11	T11	RH11	LCR11
r	-0.280	-0.242	0.685	-0.073	0.070	0.066	0.005	0.344	0.822	-0.019	0.018	0.441	0.481	-0.028	-0.071	-0.310	0.473	0.493
P	0.337	0.940	0.013	0.820	0.828	0.838	0.986	0.915	<0.01	0.953	0.955	0.518	0.113	0.929	0.8253	0.326	0.120	0.103

T, mean daily temperature; RH, mean daily relative humidity; LCR, logarithm of accumulated rainfall.

*Numbers following abbreviations of T, RH and LCR refer to the weather data summarized at 1, 2, 4, 8 and 11 weeks of the experimental periods in all seasons. Significant values ($P \leq 0.05$) are shown in bold.

Figure 1. Boxplot illustrating the differences in Chao1 **(a)** and Shannon **(b)** diversity measures of the fungal communities in the three Denominations of Origin.

Figure 2. Principal Coordinate Analysis (PCoA) based on Bray Curtis dissimilarity metrics in 3D **(a)** and 2D **(b)**, showing the distance in the fungal communities among Denominations of Origin.

Figure 3. Venn diagram illustrating the overlap of the OTUs identified in the fungal microbiota among Denominations of Origin.

Figure 4. Boxplot illustrating the differences in Chao1 and Shannon diversity measures of the fungal communities between both infection periods in D.O. Ribeiro **(a)**, D.O. Rías Baixas **(b)**, and Valdeorras **(c)**.

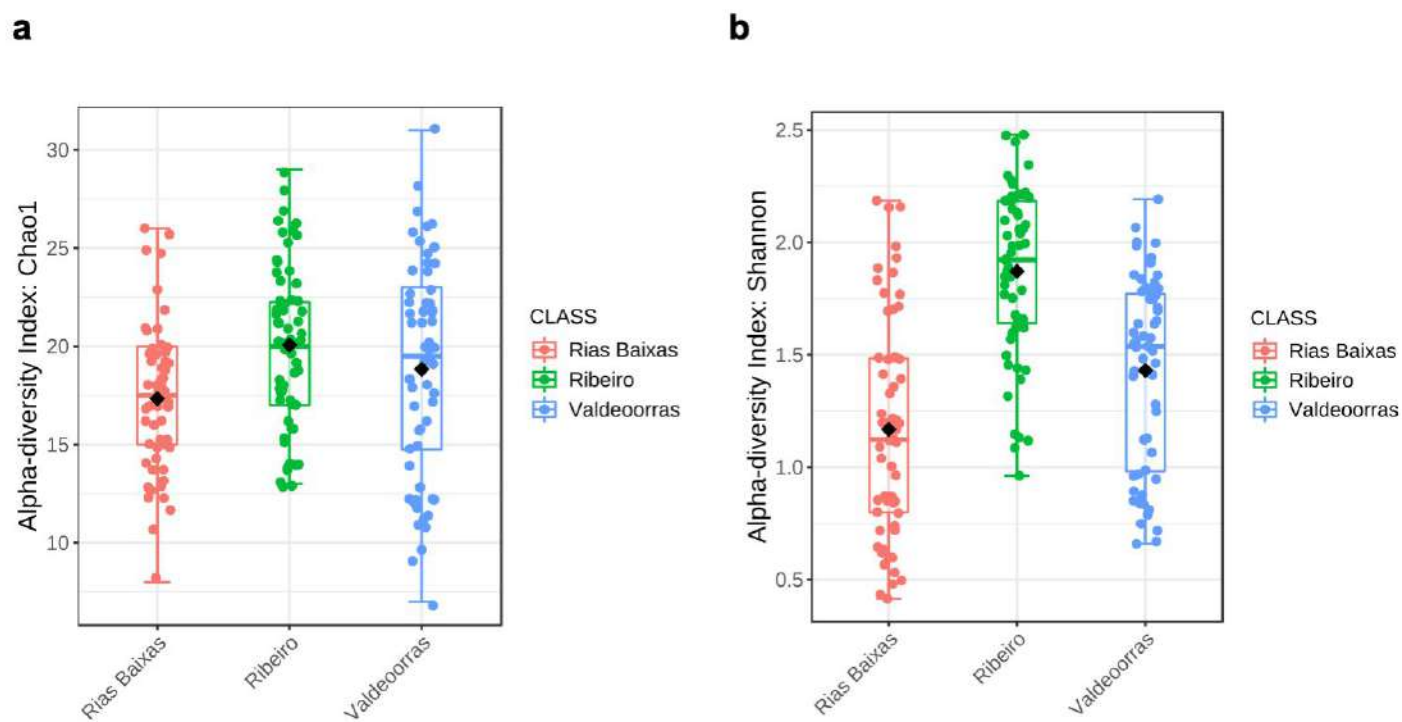
Figure 5. Relative abundance of different fungal families detected across sampling times (initial microbiome, infection period 1 and infection period 2) in D.O. Ribeiro **(a)**, D.O. Rías Baixas **(b)**, and Valdeorras **(c)**.

Figure 6. Venn diagram illustrating the overlap of the OTUs identified in the fungal microbiota among sampling times in D.O. Ribeiro **(a)**, D.O. Rías Baixas **(b)**, and Valdeorras **(c)**.

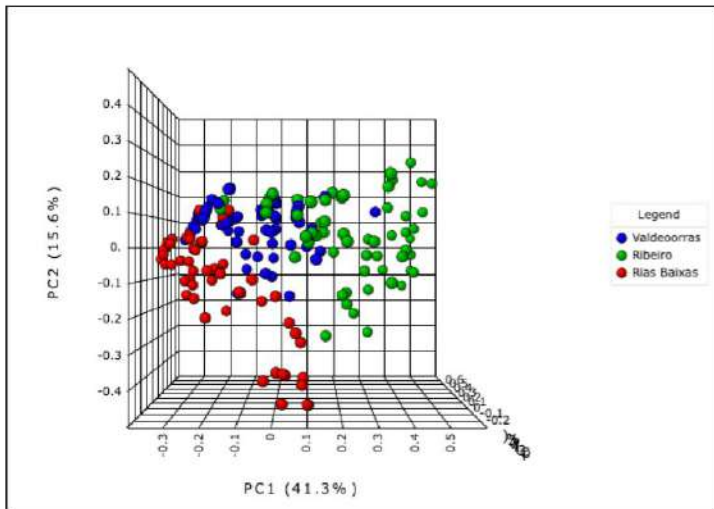
Figure 7. LEfSe was used to identify the most differentially abundant taxa between infection periods. Bar graph showing LDA scores for fungal genera. Only taxa meeting an LDA significant threshold >2 are shown.

Figure 8. Boxplot illustrating the differences in Chao1 and Shannon diversity measures of the grapevine trunk disease pathogens between both infection periods in D.O. Ribeiro **(a)**, D.O. Rías Baixas **(b)**, and Valdeorras **(c)**.

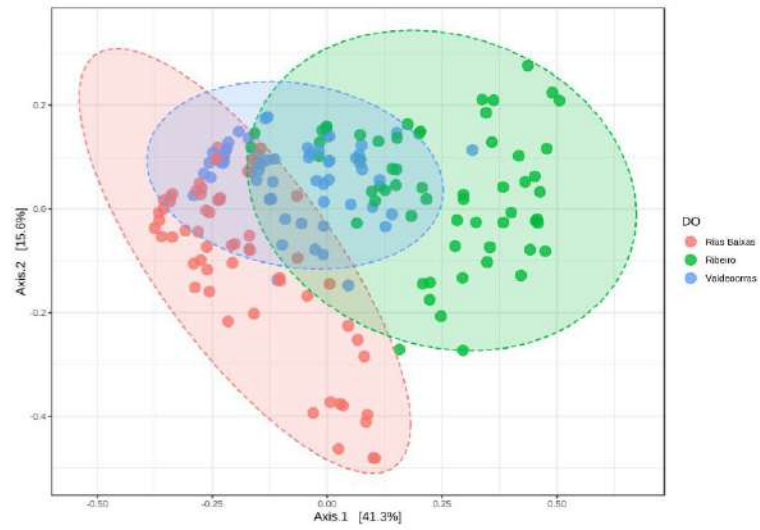
Figure 9. Distribution of the relative abundance of fungal trunk diseases genera obtained by high-throughput amplicon sequencing in both infection periods in D.O. Ribeiro **(a)**, D.O. Rías Baixas **(b)**, and Valdeorras **(c)**. Asterisks (*) indicate significant differences in fungal abundances between infection periods ($P=0.05$).

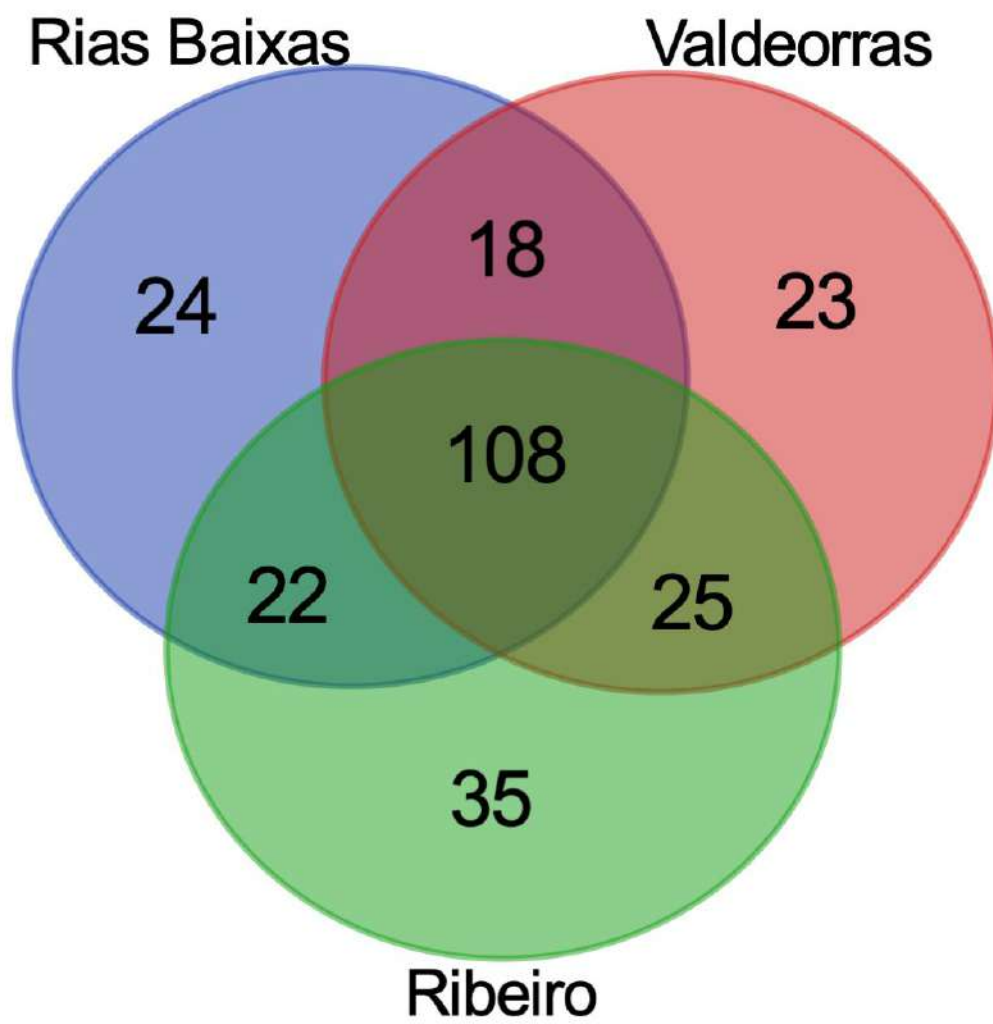


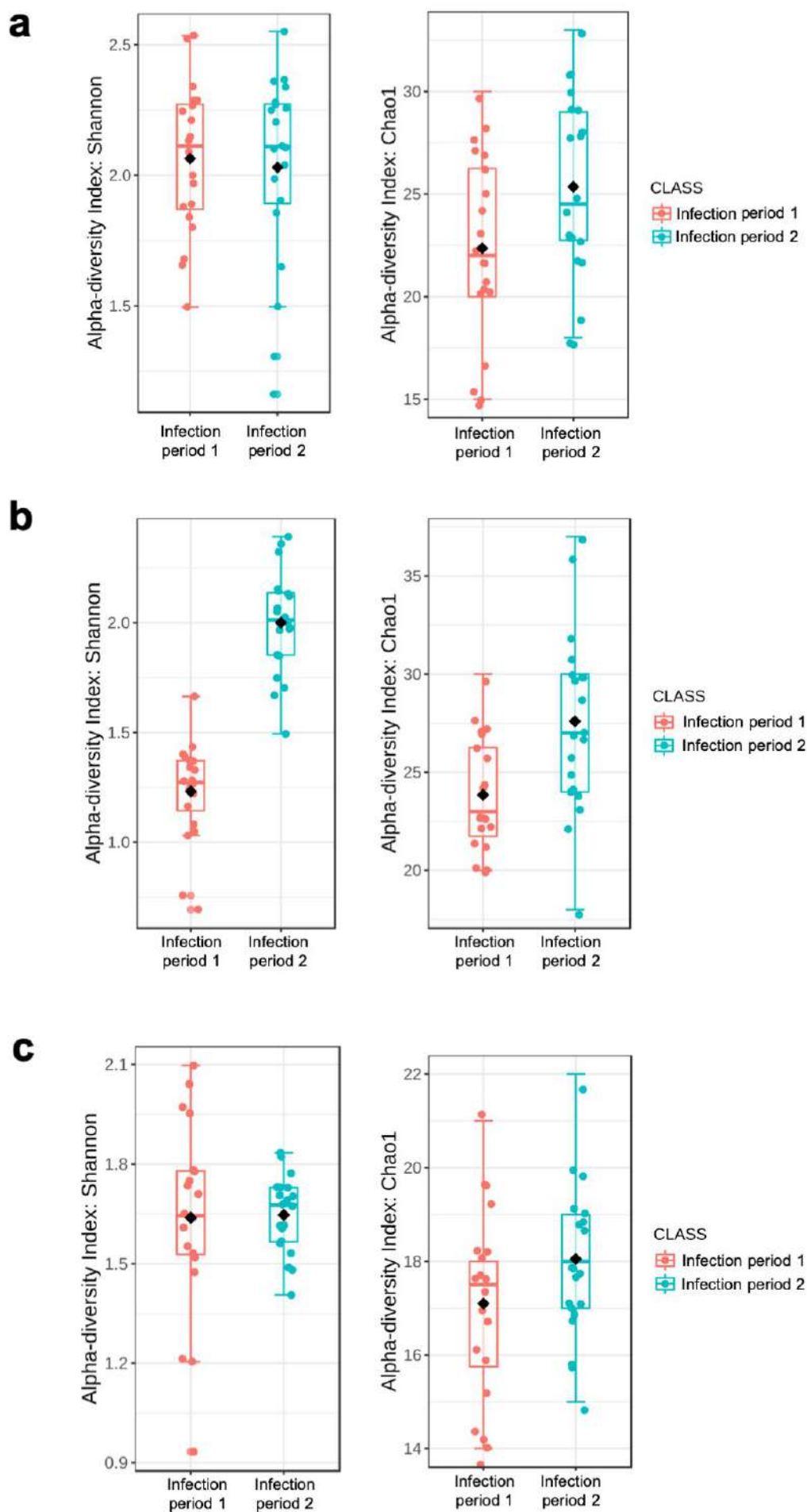
a

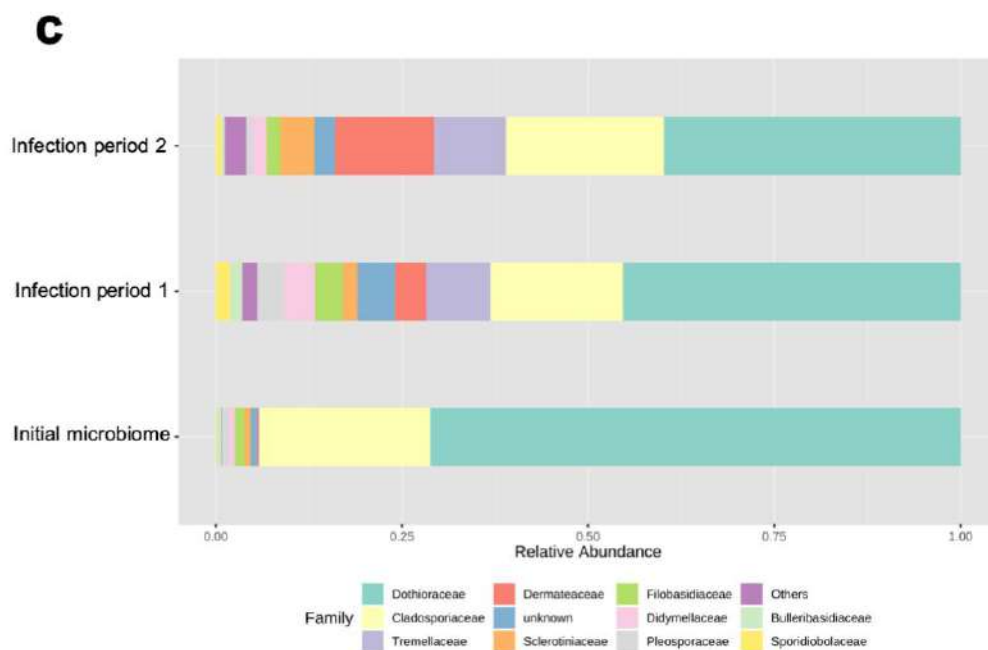
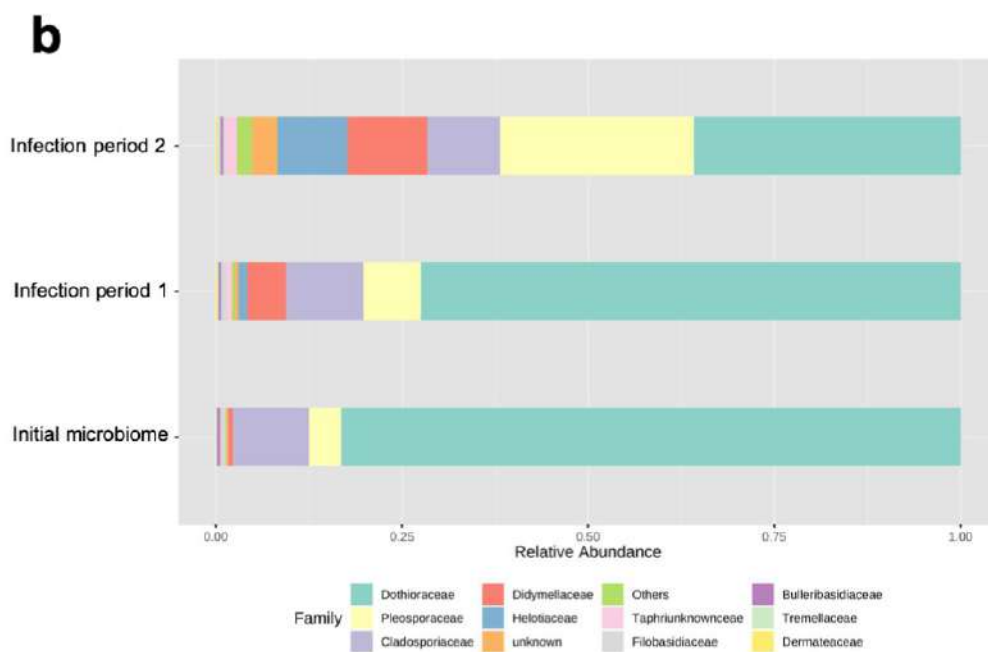
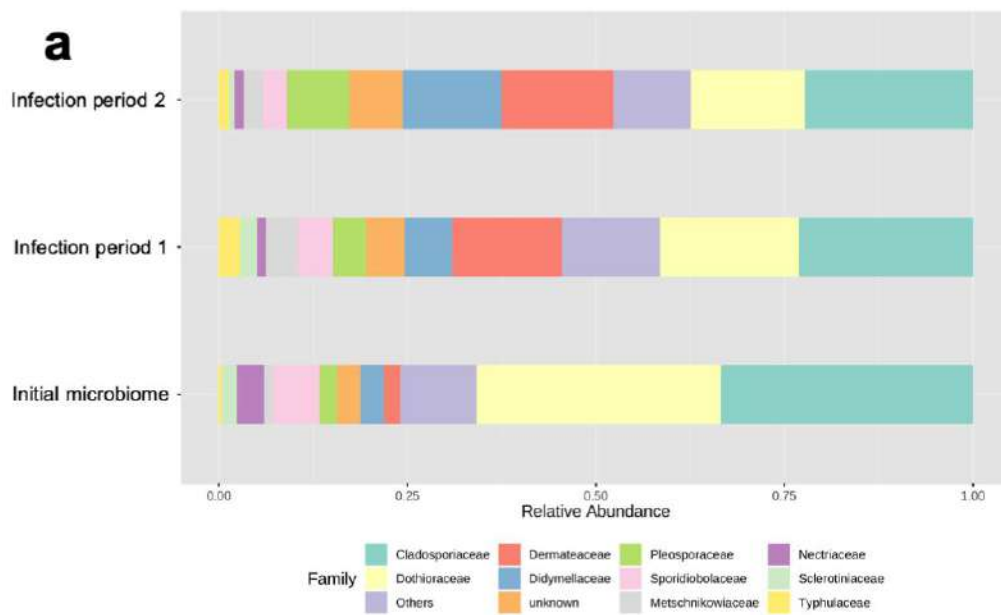


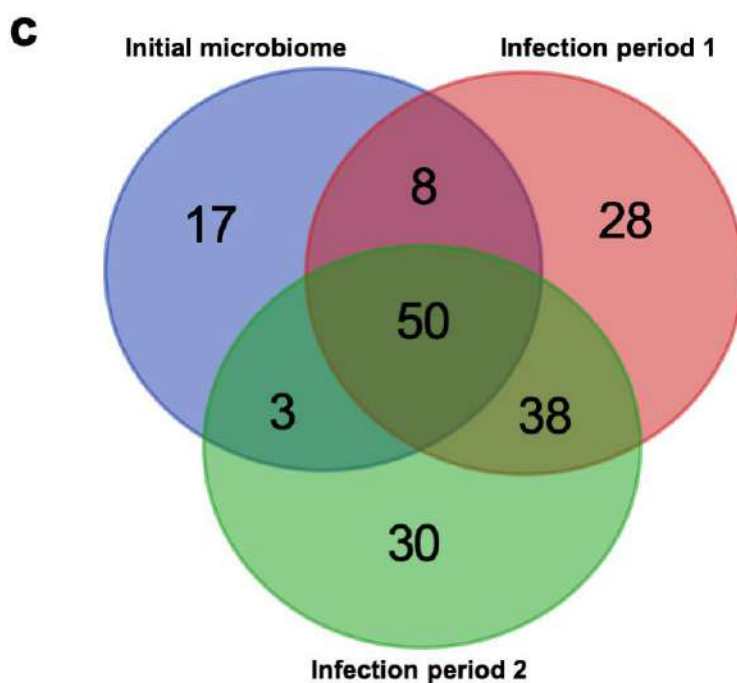
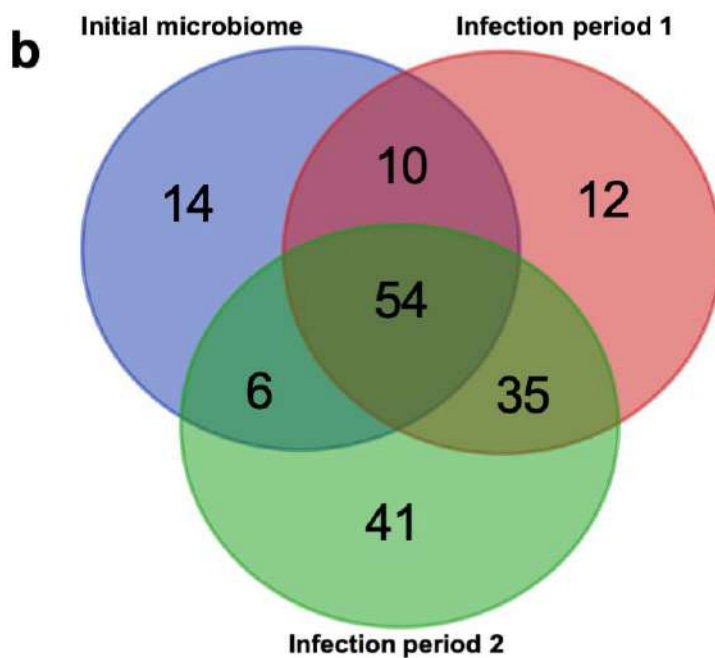
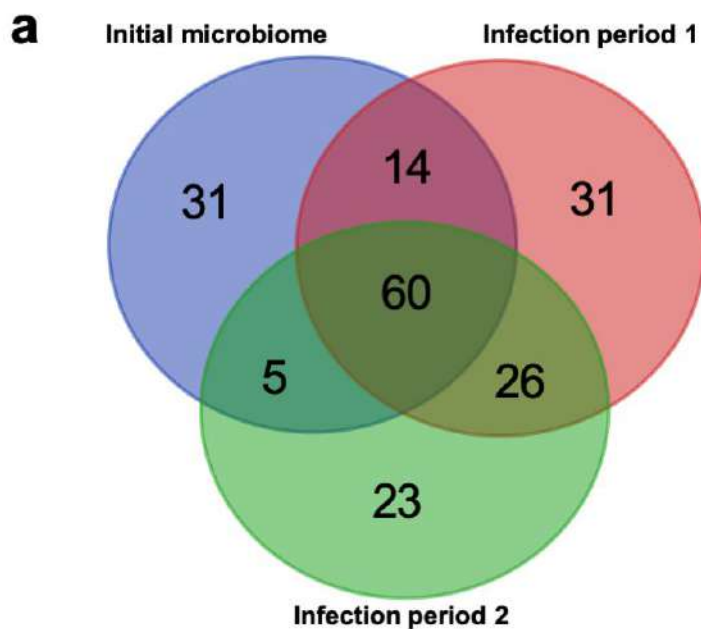
b



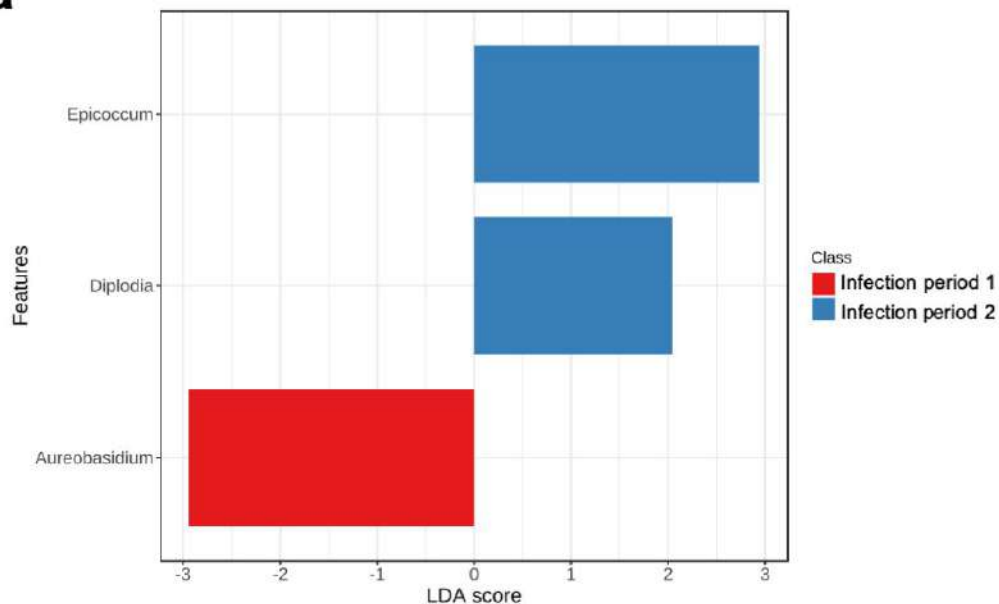




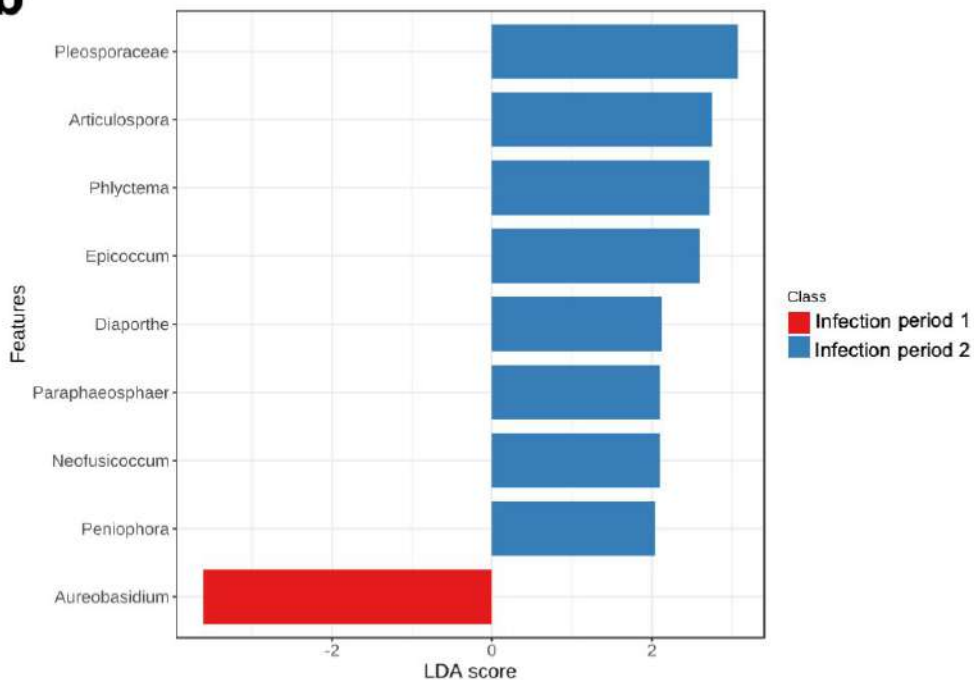




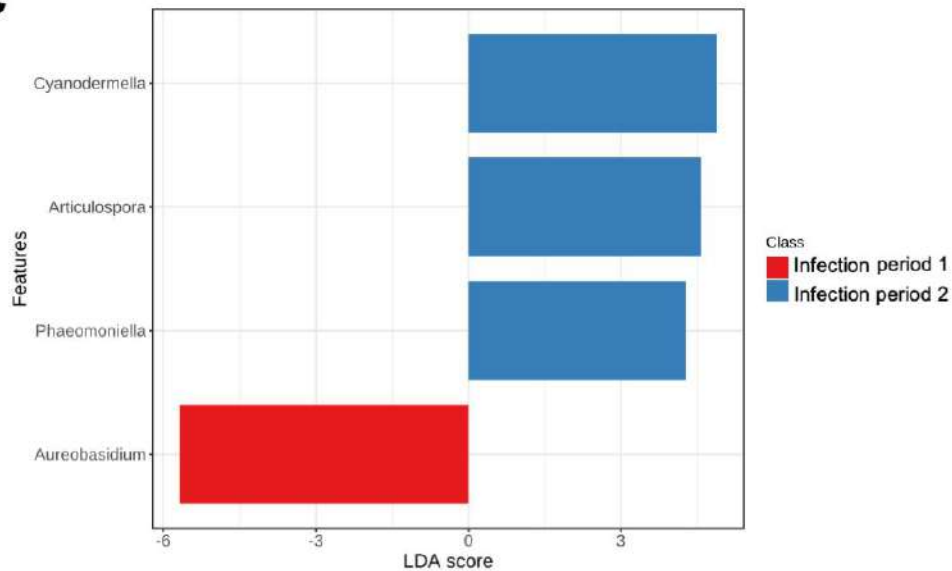
a



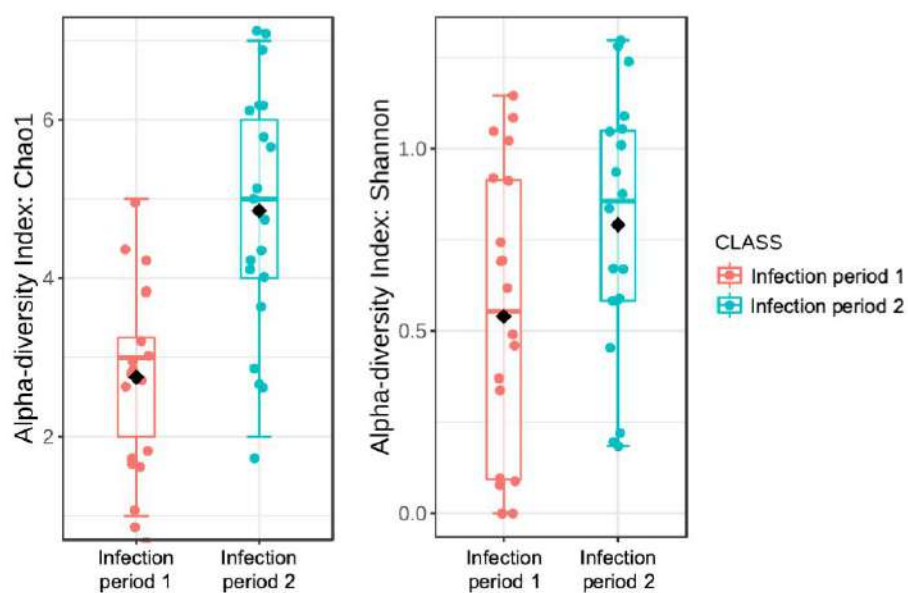
b



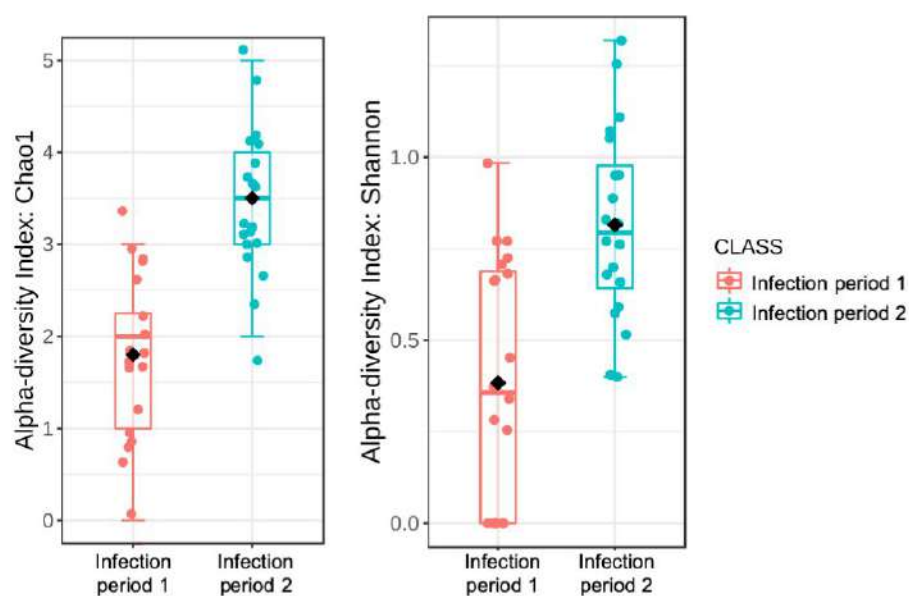
c



a



b



c

